Journal of Statistics Applications & Probability
An International Journal

http://dx.doi.org/10.18576/jsap/150605

A Novel Unit Modified Weibull Distribution: Properties, Quantile Regression and Applications

Abdul Ghaniyyu Abubakari

Department of Applied Statistics, Faculty of Social Science and Arts, University of Business and Integrated Development Studies, Wa, Ghana

Received: 10 Sep. 2026, Revised: 17 Oct. 2026, Accepted: 26 Oct. 2026
Published online: 1 Nov. 2026

Abstract: In this paper, we introduce a novel unit modified Weibull distribution for modelling data defined on the interval (0,1). Such data are recorded across disciplines ranging from engineering to the social sciences, and often exhibit skewness, outliers and non-monotone hazard rates that standard unit distributions cannot adequately capture. This has motivated the continuous development of new unit distributions for modelling complex data on the unit interval. The density of the proposed distribution can be increasing, decreasing, or unimodal with left or right skewness, while its hazard rate can exhibit monotone increasing, monotone decreasing, bathtub and modified bathtub shapes. Some properties, including quantile function, moments, stochastic ordering, order statistics and inequality measures, are derived. Also, the identifiability of its parameters is established. Maximum likelihood estimators are obtained for the parameters, and simulations reveal that the estimators are consistent and asymptotically unbiased. An alternative quantile based regression model using the proposed distribution is developed. Four real data applications demonstrate that the distribution and its regression model provide better fit than nine established distributions and four quantile regression models, respectively. The proposed methodology expands the toolkit available for unit data modeling.

Keywords: Unit distributions, modified Weibull distribution, quantile regression model, data analytics, flexible distributions.

1 Introduction

Over the last few decades, the development of unit probability distributions has gained attention due to the vital role they play in the analysis of unit interval data. Data on the unit interval are common in fields such as engineering, finance, health, actuarial science and the social sciences. This type of data comes in the form of proportions, percentages, ratios, rates, among others. Accurate analysis of such data underpins informed decision-making. This is especially important where resources are constrained, since impactful and sustainable development depends on using them well. Several distributions have been constructed for the analysis of unit interval data. Notable among them are the beta and Kumaraswamy (Kum) [1] distributions. However, data from various fields tend to exhibit varying traits, including different degrees of distributional asymmetry and tail behavior making it impracticable for traditional unit distributions, including beta and Kum distributions, to provide adequate fit. Due to this, researchers continue to develop unit distributions to accommodate the different features exhibited by unit interval data.

Some distributions on the unit bounded domain include unit Gamma [2,3], Topp-Leone (TL) [4], unit Weibull (UW) [5], unit Lindley (UL) [6], unit Rayleigh (UR) [7], unit generalized half normal [8], log-weighted exponential [9], unit exponentiated Fréchet [10], new bounded unit Weibull [11], sine-Marshall–Olkin Topp–Leone [12], log-cosine power (LCP) [13], unit Weibull loss [14], unit modified Weibull (UMW) [15], new unit Lindley (NUL) [16], log-Lindley exponential [17], power unit Haq [18], unit Jamal [19] and power-transformed Bradford [20] distributions. Others include the Epanechnikov power unit inverse Lindley [21], unit Zeghdoudi [22], unit power Rayleigh [23], transmuted unit new XLindley [24], unit Komal [25] and unit ZLindley [26] distributions. For a review of unit distributions, refer to [27].

The UMW distribution [15] is derived from the modified Weibull (MW) distribution [28]. The MW distribution is an attractive baseline as it accommodates increasing, decreasing and bathtub shaped hazard rates. In UMW distribution,

* Corresponding author e-mail: abughaniyyu@gmail.com

© 2026 NSP
Natural Sciences Publishing Cor.

however, the behaviour of its density and hazard rate is determined by a single shape parameter. This limits how adequately the distribution fits complex data. To overcome this, a new unit distribution, called the novel unit modified Weibull (NUMW) distribution, is developed in this study. It is obtained from the MW distribution through a power transformation that adds an extra parameter. The NUMW distribution contains the UMW distribution as a special case, and its density and hazard shapes are governed by the product of two parameters rather than one.

In statistical modeling, regression models play an important role in determining the effect of a set of covariates on a response variable. Classical regression models relate the conditional mean of response variables to covariates. Though several regression models based on the conditional mean have been developed, there are situations where response variables are characterized by asymmetry or outliers, making the conditional mean unsuitable for the data. Quantile regression (QR) models, developed by [29], are more robust in such situations. QR models relate the conditional quantiles of the response to the set of regressors. Several researchers have developed QR models for unit bounded response variable. Among these models are Kumaraswamy QR (KQR) [30], log-extended exponential-geometric QR (LEEGQR) [31], unit-Generalized Half-Normal-X QR (UGHNXQR) [32], Vasicek QR [33], unit exponentiated Fréchet QR [10], unit-Gompertz QR (UGQR) [34], unit Weibull loss QR [14], unit modified Weibull QR [15], new bounded unit Weibull QR [11] and power-transformed Bradford QR [20] models. Others include unit Gumbel-logistic QR [35], unit-Cauchy QR [36], unit extended exponential geometric QR [37], unit Chen QR [38] and unit exponential QR [39] models. A QR model built on the NUMW distribution inherits the desirable features of the distribution, making it more suitable for describing the conditional distribution of the response variable.

The key contributions of this study are fourfold:

1. Development of a new four-parameter flexible unit distribution, capable of modelling data exhibiting various features. The UMW distribution is contained as a special case.
2. Derivation of properties of the new unit distribution, illustrated numerically and graphically.
3. A QR model that inherits the flexibility of the new distribution is developed for measuring the relationship between unit bounded responses and covariates.
4. Using four real datasets, the NUMW distribution and its associated QR model are compared with nine competing distributions and four competing QR models.

The subsequent sections of the article proceed as follows: The development of the new distribution is presented in Section 2, with the identifiability of its parameters. Section 3 presents numerous distributional properties of the new distribution. Maximum likelihood technique is used to estimate the parameters of the distribution and presented in Section 4. Furthermore, simulation studies are used to assess the behavior of the estimators. QR model for the new distribution is developed in Section 5. Data analysis is carried out in Section 6 to showcase the potentials of the distribution and its regression model. The conclusions of the study, alongside some recommendations for future studies, are presented in Section 7.

2 Novel Unit Modified Weibull Distribution

The NUMW distribution is developed in this section. Let X follow the MW distribution [28] with cumulative distribution function (CDF) and associated probability density function (PDF) given, respectively, as

$$F_X(x) = 1 - e^{-\varphi x^{\rho} e^{\varsigma x}},\ \varphi, \rho, \varsigma > 0, x \geq 0 \tag{1}$$

and

$$f_X(x) = \varphi(\rho + \varsigma x) x^{\rho-1} e^{\varsigma x} e^{-\varphi x^{\rho} e^{\varsigma x}},\ x \geq 0. \tag{2}$$

Given that $W = 1 - (1 - e^{-X})^{\frac{1}{\vartheta}}$, $\vartheta > 0$, then $X \in (0, \infty)$ is mapped onto the unit interval $W \in (0,1)$. Thus, $X = -\ln\left[1 - (1-W)^{\vartheta}\right]$ and $\frac{dX}{dW} = -\frac{\vartheta(1-W)^{\vartheta-1}}{1-(1-W)^{\vartheta}}$. Applying the transformation above, the random variable W follows the NUMW distribution with CDF derived as follows:

$$F_W(w) = \mathbb{P}(W \leq w) = \mathbb{P}\left(1 - (1 - e^{-X})^{\frac{1}{\vartheta}} \leq w\right). \tag{3}$$

Simplifying gives

$$F_W(w) = 1 - \mathbb{P}\left(X \leq -\ln\left[1 - (1-w)^{\vartheta}\right]\right) \tag{4}$$

$$= 1 - F_X\left(-\ln\left[1 - (1-w)^{\vartheta}\right]\right). \tag{5}$$

© 2026 NSP
Natural Sciences Publishing Cor.

Substituting equation (1) into (5) gives the CDF of the NUMW distribution as

$$F(w) = \exp\left(-\varphi\left[-\ln\left(1-(1-w)^{\vartheta}\right)\right]^{\rho}\left[1-(1-w)^{\vartheta}\right]^{-\varsigma}\right),\ \varphi,\rho,\varsigma,\vartheta>0, w\in(0,1). \tag{6}$$

For the rest of this paper, let $u = 1-(1-w)^{\vartheta}$, where $w \in (0,1)$, so that $u \in (0,1)$. Hence, the CDF in equation (6) can be written as

$$F(w) = \exp\left(-\varphi(-\ln u)^{\rho}u^{-\varsigma}\right),\ w\in(0,1). \tag{7}$$

The corresponding PDF of the NUMW distribution is derived by using the following transformation:

$$f_W(w) = f_X(-\ln u)\left|\frac{dX}{dW}\right|.$$

Substituting the required terms and using the PDF of the MW distribution given in equation (2) and simplifying, gives the PDF of the NUMW distribution as

$$f(w) = \frac{\varphi\vartheta(1-w)^{\vartheta-1}(\rho+\ln u^{-\varsigma})(-\ln u)^{\rho-1}}{u^{\varsigma+1}\exp(\varphi(-\ln u)^{\rho}u^{-\varsigma})},\ w\in(0,1). \tag{8}$$

The hazard rate function (HRF) of the NUMW distribution is obtained as

$$k(w) = \frac{\varphi\vartheta(1-w)^{\vartheta-1}(\rho+\ln u^{-\varsigma})(-\ln u)^{\rho-1}}{u^{\varsigma+1}[\exp(\varphi(-\ln u)^{\rho}u^{-\varsigma})-1]},\ w\in(0,1). \tag{9}$$

When $\vartheta = 1$, the NUMW distribution reduces to the UMW distribution.

The limiting behaviour of the PDF is examined as follows. Noting that $u = 1-(1-w)^{\vartheta}$ and let $v = -\ln u$.

- As $w \to 0^+$, $u \sim \vartheta w$ and $v \to \infty$. The exponential factor still dominates the remaining factors in the PDF. Hence,

$$\lim_{w\to 0^+} f(w) = 0.$$

- As $w \to 1^-$, let $x = 1-w$. Then $u = 1-x^{\vartheta} \to 1$ and $v \sim x^{\vartheta}$. Substituting these into the density gives

$$f(w) \sim \varphi\vartheta\rho x^{\vartheta\rho-1} = \varphi\vartheta\rho(1-w)^{\vartheta\rho-1}.$$

Therefore, for $\varphi,\vartheta,\rho,\varsigma>0$,

$$\lim_{w\to 1^-} f(w) = \begin{cases} 0, & \vartheta\rho>1,\\ \varphi\vartheta\rho, & \vartheta\rho=1,\\ +\infty, & \vartheta\rho<1. \end{cases} \tag{10}$$

As noted in the previous section, a weakness of the UMW distribution [15] is that the shapes of its density and hazard rate are controlled by the single parameter ρ. This limits its ability to model data exhibiting complex characteristics. The NUMW distribution addresses this limitation through the additional parameter ϑ, which adds flexibility to the distribution.

To assess the flexibility of the NUMW distribution, plots of the PDF and HRF are displayed in Figure 1 for various combinations of parameter values. It can be observed that the PDF of the NUMW distribution exhibits various shapes including left and right skewness, increasing and decreasing, and almost symmetric shapes. Also, the HRF shows bathtub, modified bathtub, increasing and decreasing shapes. These show that the NUMW distribution is flexible.

© 2026 NSP
Natural Sciences Publishing Cor.

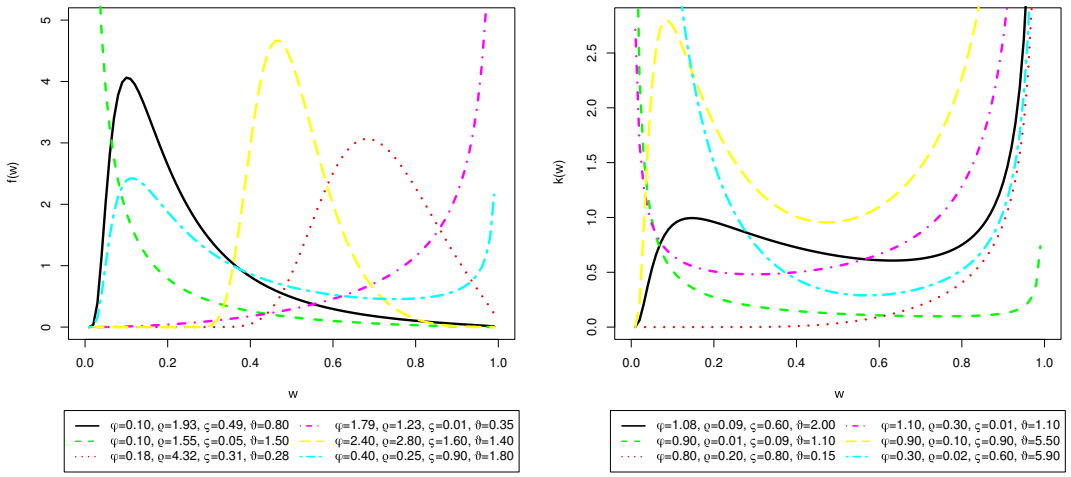


Fig. 1: PDF (left) and HRF (right) Plots of NUMW Distribution

An expansion of the PDF of the NUMW distribution is obtained for theoretical analysis of the new distribution. Firstly, the expansion of the CDF of the NUMW distribution is obtained. Using the Taylor series expansion, defined as $e^{-z} = \sum_{i=0}^{\infty}(-1)^i \frac{z^i}{i!}$, gives the CDF in equation (7) as

$$F(w) = \sum_{i=0}^{\infty} \frac{(-1)^i}{i!} \varphi^i (-\ln u)^{i\rho} u^{-i\varsigma}. \tag{11}$$

Using the expansion $-\ln(1-a) = \sum_{m=0}^{\infty} \frac{a^{(m+1)}}{m+1}$, $|a| < 1$, gives

$$-\ln\left[1-(1-w)^{\vartheta}\right] = \sum_{m=0}^{\infty} \frac{(1-w)^{\vartheta(m+1)}}{m+1}, \ |(1-w)^{\vartheta}| < 1.$$

For $i\rho > 0$, using the power series expansion in [40] gives

$$\begin{aligned}[-\ln u]^{i\rho} &= \left(\sum_{m=0}^{\infty} \frac{(1-w)^{\vartheta(m+1)}}{m+1}\right)^{i\rho} \\ &= \sum_{k=0}^{\infty} C_k (1-w)^{\vartheta(i\rho+k)},\end{aligned}$$

where $C_0 = 1$ and $C_k = \frac{1}{k}\sum_{j=1}^{k} \frac{[j(i\rho+1)-k]}{j+1} C_{k-j}$. This gives equation (11) as

$$F(w) = \sum_{i=0}^{\infty}\sum_{k=0}^{\infty} \frac{(-1)^i}{i!} \varphi^i C_k (1-w)^{\vartheta(i\rho+k)} u^{-i\varsigma}. \tag{12}$$

Further using the generalized binomial expansion gives

$$\left[1-(1-w)^{\vartheta}\right]^{-i\varsigma} = \sum_{l=0}^{\infty} \binom{i\varsigma+l-1}{l} (1-w)^{\vartheta l}.$$

This expansion gives the CDF of the NUMW distribution as

$$F(w) = \sum_{i=0}^{\infty}\sum_{k=0}^{\infty}\sum_{l=0}^{\infty} \binom{i\varsigma+l-1}{l} \frac{(-1)^i}{i!} \varphi^i C_k (1-w)^{\vartheta(i\rho+k+l)}. \tag{13}$$

Letting

$$\Delta_{kl}^{*} = \sum_{k=0}^{\infty}\sum_{l=0}^{\infty} \binom{i\varsigma+l-1}{l} \frac{(-1)^i}{i!} C_k$$

© 2026 NSP
Natural Sciences Publishing Cor.

gives the CDF of the NUMW distribution as

$$F(w) = \sum_{i=0}^{\infty} \Delta_{kl}^{*} \varphi^{i} (1-w)^{\vartheta(i\rho+k+l)}. \tag{14}$$

Differentiating equation (14) gives the PDF of the NUMW distribution as

$$f(w) = \sum_{i=0}^{\infty} \Delta_{kl} \varphi^{i} \vartheta (i\rho+k+l)(1-w)^{\vartheta(i\rho+k+l)-1}, \tag{15}$$

where $\Delta_{kl} = -\Delta_{kl}^{*}$.

2.1 Identifiability of Parameters

The identifiability of the parameters of the NUMW distribution is presented in this subsection. This is necessary for reliability in estimators as it ensures their uniqueness.

Let $\Theta = (\varphi, \rho, \varsigma, \vartheta)$ be the parameter vector of the distribution. Given two sets of parameter vectors from the NUMW distribution as $\Theta_k = (\varphi_k, \rho_k, \varsigma_k, \vartheta_k), k = 1,2$. The NUMW distribution is identifiable if $F(w;\Theta_1) = F(w;\Theta_2)\ \forall w \in (0,1)$ implies $\Theta_1 = \Theta_2$.

Let $u_k(w) = 1-(1-w)^{\vartheta_k}$ and $G_k(w) = \varphi_k \left[-\ln u_k(w)\right]^{\rho_k} \left[u_k(w)\right]^{-\varsigma_k}$ for $k = 1,2$. This gives the CDF in equation (7) as $F(w) = \exp(-G_k(w))$. For $w \in (0,1)$, we have $0 < u_k(w) < 1$, so $-\ln u_k(w) > 0$ and $G_k(w) > 0$. Because the exponential function is injective, equality of the two CDFs implies equality of the two exponents. That is,

$$\varphi_1 \left[-\ln u_1(w)\right]^{\rho_1} \left[u_1(w)\right]^{-\varsigma_1} = \varphi_2 \left[-\ln u_2(w)\right]^{\rho_2} \left[u_2(w)\right]^{-\varsigma_2} \quad \forall w \in (0,1). \tag{16}$$

Note that both sides of (16) are positive. Hence, taking logarithms of both sides give

$$\ln G_k(w) = \ln \varphi_k + \rho_k \ln[-\ln u_k(w)] - \varsigma_k \ln u_k(w), \quad k = 1,2. \tag{17}$$

Equation (16) is now examined near the two endpoints of the interval $(0,1)$.

- $w \to 0^{+}$: A first-order expansion gives $(1-w)^{\vartheta_k} = 1 - \vartheta_k w + O(w^2)$. Hence, as $w \to 0^{+}$, we have

$$u_k(w) = \vartheta_k w \{1 + O(w)\}. \tag{18}$$

Taking the negative logarithm of both sides of equation (18) yields

$$\begin{aligned} -\ln u_k(w) &= -\ln w - \ln \vartheta_k + o(1) \\ &= -\ln w \left(1 + \frac{-\ln \vartheta_k + o(1)}{-\ln w}\right). \end{aligned} \tag{19}$$

Further taking logarithms of both sides of equation (19) gives

$$\ln\left[-\ln u_k(w)\right] = \ln\left[-\ln w \left(1 + \frac{-\ln \vartheta_k + o(1)}{-\ln w}\right)\right] \tag{20}$$

$$= \ln(-\ln w) + \ln\left(1 + \frac{-\ln \vartheta_k + o(1)}{-\ln w}\right). \tag{21}$$

Since $-\ln w \to \infty$ as $w \to 0^{+}$, the constant $-\ln \vartheta_k$ is negligible relative to $-\ln w$, and therefore, equation (21) becomes

$$\ln\left[-\ln u_k(w)\right] = \ln(-\ln w) + o(1). \tag{22}$$

Substituting the expansions in equations (18) and (22) into equation (17) for $k = 1,2$, and simplifying gives

$$-\varsigma_1 \ln w + \rho_1 \ln(-\ln w) + \ln\left(\varphi_1 \vartheta_1^{-\varsigma_1}\right) + o(1) = -\varsigma_2 \ln w + \rho_2 \ln(-\ln w) + \ln\left(\varphi_2 \vartheta_2^{-\varsigma_2}\right) + o(1). \tag{23}$$

The three terms on each side of equation (23) grow at different rates. That is $-\ln w \to \infty$, $\ln(-\ln w) \to \infty$ much more slowly, and the third term is bounded. Their coefficients can therefore be compared one at a time. Dividing both sides of equation (23) by $-\ln w$ gives

$$\varsigma_1 + \frac{\rho_1 \ln(-\ln w)}{-\ln w} + \frac{\ln\left(\varphi_1 \vartheta_1^{-\varsigma_1}\right)}{-\ln w} + o(1) = \varsigma_2 + \frac{\rho_2 \ln(-\ln w)}{-\ln w} + \frac{\ln\left(\varphi_2 \vartheta_2^{-\varsigma_2}\right)}{-\ln w} + o(1).$$

Now, letting $w \to 0^{+}$ gives $\varsigma_1 = \varsigma_2$. With $\varsigma_1 = \varsigma_2$, the leading terms of equation (23) cancel. Dividing what remains by $\ln(-\ln w)$ and letting $w \to 0^{+}$ gives $\rho_1 = \rho_2$.

© 2026 NSP
Natural Sciences Publishing Cor.

- $w \to 1^-$: Let $x = 1-w$, so that $x \to 0^+$ as $w \to 1^-$. This gives $u_k = 1 - x^{\vartheta_k} \to 1$. Applying the expansion $-\ln(1-s) = s + O(s^2)$ as $s \to 0$, with $s = x^{\vartheta_k}$, gives

$$-\ln u_k = -\ln\left(1 - x^{\vartheta_k}\right) \sim x^{\vartheta_k}.$$

Again, $u_k^{-\varsigma_k} = (1-x^{\vartheta_k})^{-\varsigma_k} \to 1$. Consequently, as $x \to 0^+$

$$G_k(w) \sim \varphi_k x^{\vartheta_k \rho_k}.$$

Taking logarithms and dividing by $\ln x$, noting that $\ln x \to -\infty$ as $x \to 0^+$, gives

$$\lim_{x\to 0^+} \frac{\ln G_k(w)}{\ln x} = \vartheta_k \rho_k.$$

Since $G_1(w) = G_2(w)\ \forall w$, these limits are equal, and so $\vartheta_1\rho_1 = \vartheta_2\rho_2$. It is already shown that $\rho_1 = \rho_2$. Dividing by ρ gives $\vartheta_1 = \vartheta_2$. At this stage ϑ, ρ and ς are known to be the same for both parameter sets. Writing ϑ, ρ, ς for these common parameters, then equation (16) becomes

$$\varphi_1 \left[-\ln u\right]^{\rho} u^{-\varsigma} = \varphi_2 \left[-\ln u\right]^{\rho} u^{-\varsigma}. \tag{24}$$

Dividing through by the common factor, gives $\varphi_1 = \varphi_2$.

Combining the four equalities of the parameters, it can be concluded that

$$\Theta_1 = (\varphi_1, \rho_1, \varsigma_1, \vartheta_1) = (\varphi_2, \rho_2, \varsigma_2, \vartheta_2) = \Theta_2.$$

Hence distinct parameter vectors yield distinct distributions, and the distribution is identifiable.

3 Distributional Properties

The distributional properties of the NUMW distribution are derived in the present section. The quantile function (QF), moments, stochastic ordering, order statistics and inequality measures are presented for the distribution.

3.1 Quantile Function

For the generation of random samples from the NUMW distribution, its QF is required. Again, the QF can be used to obtain the distributional features of the distribution. The QF of a continuous distribution is the inverse function of its CDF. Given that $\tau \in (0,1)$, the QF of the NUMW distribution is obtained by letting equation (7) be equal to τ gives

$$\exp\left(-\varphi(-\ln u)^{\rho} u^{-\varsigma}\right) = \tau.$$

Simplifying gives

$$(-\ln u)^{\rho} u^{-\varsigma} = -\frac{\ln(\tau)}{\varphi}.$$

Raising both sides of the equation to the power $\frac{1}{\rho}$ gives

$$(-\ln u) u^{-\frac{\varsigma}{\rho}} = \left(-\frac{\ln(\tau)}{\varphi}\right)^{\frac{1}{\rho}}.$$

Noting that $u^{-\frac{\varsigma}{\rho}} = \exp\left(-\frac{\varsigma}{\rho}\ln u\right)$ and multiplying both sides by $\frac{\varsigma}{\rho}$ gives

$$\left[-\frac{\varsigma}{\rho}\ln u\right] \exp\left(-\frac{\varsigma}{\rho}\ln u\right) = \frac{\varsigma}{\rho}\left(-\frac{\ln(\tau)}{\varphi}\right)^{\frac{1}{\rho}}$$

© 2026 NSP
Natural Sciences Publishing Cor.

Applying Lambert function, defined as $\mathbb{W}(xe^x) = x$, to both sides gives

$$-\frac{\varsigma}{\rho}\ln u = \mathbb{W}\left[\frac{\varsigma}{\rho}\left(-\frac{\ln(\tau)}{\varphi}\right)^{\frac{1}{\rho}}\right].$$

Simplifying,

$$\ln u = -\frac{\rho}{\varsigma}\mathbb{W}\left[\frac{\varsigma}{\rho}\left(-\frac{\ln(\tau)}{\varphi}\right)^{\frac{1}{\rho}}\right].$$

Recalling that $u = 1-(1-w)^{\vartheta}$, further simplifying and making w the subject gives the QF of the NUMW distribution as

$$Q_W(\tau) = 1-\left[1-\exp\left(-\frac{\rho}{\varsigma}\mathbb{W}\left[\frac{\varsigma}{\rho}\left(-\frac{\ln(\tau)}{\varphi}\right)^{\frac{1}{\rho}}\right]\right)\right]^{\frac{1}{\vartheta}}, \quad \tau \in (0,1). \tag{25}$$

The median of the NUMW distribution can be obtained by setting τ to 0.5 in equation (25). This gives

$$Q_W(0.5) = 1-\left[1-\exp\left(-\frac{\rho}{\varsigma}\mathbb{W}\left[\frac{\varsigma}{\rho}\left(\frac{\ln(2)}{\varphi}\right)^{\frac{1}{\rho}}\right]\right)\right]^{\frac{1}{\vartheta}}. \tag{26}$$

Bowley's skewness and Moors' kurtosis can be used to examine the skewness and kurtosis of the NUMW distribution. These measures are based on the QF and defined as

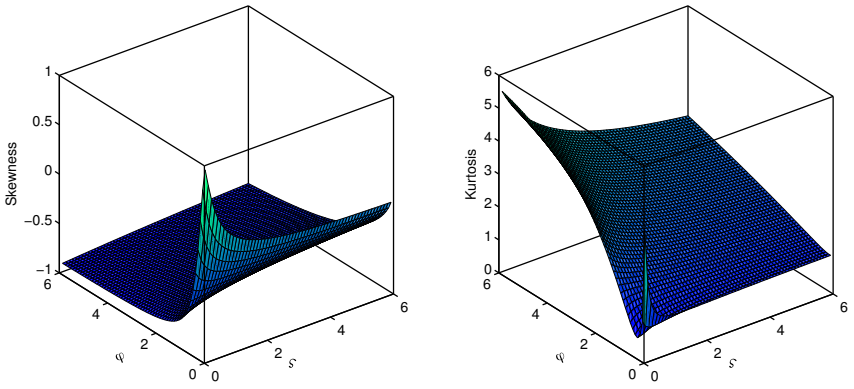
$$\text{Bowley Skewness} = \frac{Q_W\left(\frac{3}{4}\right)+Q_W\left(\frac{1}{4}\right)-2Q_W\left(\frac{2}{4}\right)}{Q_W\left(\frac{3}{4}\right)-Q_W\left(\frac{1}{4}\right)}$$

and

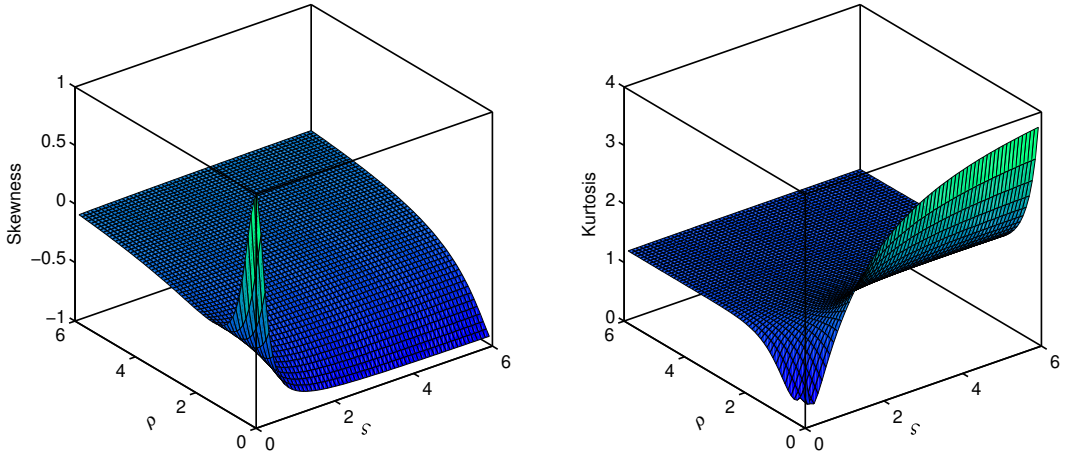
$$\text{Moors Kurtosis} = \frac{Q_W\left(\frac{7}{8}\right)-Q_W\left(\frac{5}{8}\right)+Q_W\left(\frac{3}{8}\right)-Q_W\left(\frac{1}{8}\right)}{Q_W\left(\frac{6}{8}\right)-Q_W\left(\frac{2}{8}\right)}.$$

Figure 2 illustrates the plots of skewness and kurtosis for some selected pairs of fixed values. These include $(\rho = 0.7, \vartheta = 0.3)$, $(\varphi = 0.3, \vartheta = 0.13)$ and $(\varphi = 0.9, \varsigma = 0.1)$. For each pair, the remaining parameters vary over a range of values. The distribution exhibits varying levels of kurtosis. Also, different degrees of skewness including symmetric, positively and negatively skewed shapes are observed.

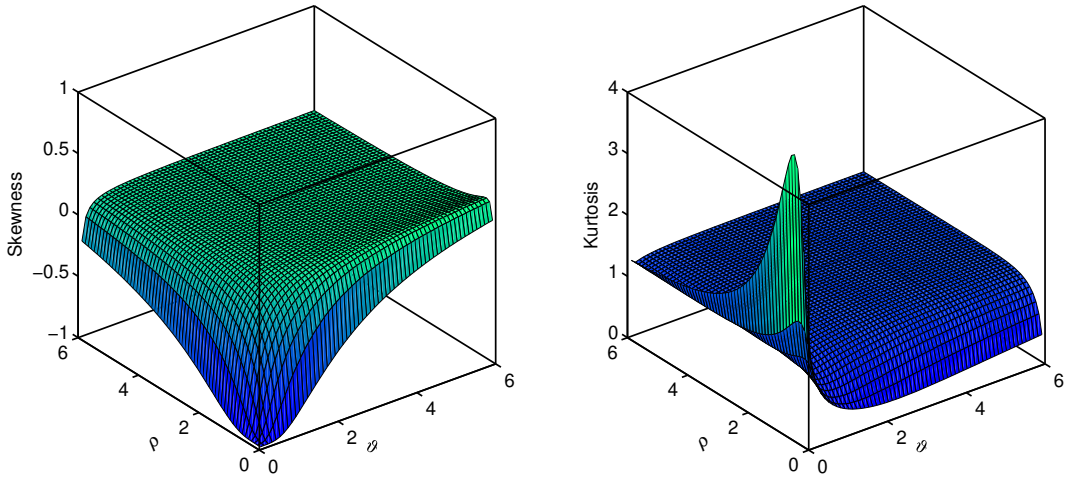
© 2026 NSP
Natural Sciences Publishing Cor.



(a) $\rho = 0.7, \vartheta = 0.3$



(b) $\varphi = 0.3, \vartheta = 0.13$



(c) $\varphi = 0.9, \varsigma = 0.1$

Fig. 2: Skewness and Kurtosis Plots of NUMW Distribution

© 2026 NSP
Natural Sciences Publishing Cor.

3.2 Moments

The ordinary, central, and incomplete moments of the NUMW distribution, together with its moment generating function, are derived in this section. These characterizations are useful for describing the NUMW distribution.

3.2.1 Ordinary Moments

The rth ordinary moment of the NUMW distribution is obtained by evaluating the equation $\mu'_r = \int_0^1 w^r f(w)dw,\ r = 1,2,3,\ldots$. Substituting equation (15) into the definition gives

$$\mu'_r = \sum_{i=0}^{\infty} \Delta_{kl} \varphi^i \vartheta(i\rho + k + l) \int_0^1 w^r (1-w)^{\vartheta(i\rho+k+l)-1} dw. \tag{27}$$

Using the beta function, defined as $\mathbb{B}(a,b) = \int_0^1 w^{a-1}(1-w)^{b-1}dw$, gives the moment as

$$\mu'_r = \sum_{i=0}^{\infty} \Delta_{kl} \varphi^i \vartheta(i\rho + k + l) \mathbb{B}\left(r+1, \vartheta(i\rho+k+l)\right),\ \ r = 1,2,3,\ldots. \tag{28}$$

Setting r to 1, 2, 3 and 4, various moments can be obtained. The central moments of the NUMW distribution can be obtained using the relationship

$$\mu_n = \mathbb{E}\left[(W-\mu)^n\right] = \sum_{k=0}^{n} \binom{n}{k} (-1)^k \mu^k \mu'_{n-k}, \tag{29}$$

where $\mu = \mu'_1$ is the mean and μ'_{n-k} is the $(n-k)$th ordinary moment of the distribution. The coefficient of skewness (CS) and kurtosis (CK) are obtained using the following respective formulas: CS $= \frac{\mu'_3 - 3\mu'_2\mu'_1 + 2\mu'^3_1}{\left(\mu'_2 - \mu'^2_1\right)^{3/2}}$, and CK $= \frac{\mu'_4 - 4\mu'_3\mu'_1 + 6\mu'_2\mu'^2_1 - 3\mu'^4_1}{\left(\mu'_2 - \mu'^2_1\right)^2}$.

Table 1 reports the first four ordinary moments, the second, third and fourth central moments, CS and CK of the NUMW distribution. The following four different parameter sets are used for the computation: $P_1 = (\varphi = 0.1, \rho = 0.5, \varsigma = 7.1, \vartheta = 4.3)$, $P_2 = (\varphi = 1.1, \rho = 1.2, \varsigma = 2.9, \vartheta = 1.9)$, $P_3 = (\varphi = 0.8, \rho = 0.2, \varsigma = 0.4, \vartheta = 0.8)$ and $P_4 = (\varphi = 0.2, \rho = 1.6, \varsigma = 3.5, \vartheta = 0.2)$. It can be observed that the findings of the moment based measures confirm the observations made using the quantile based measures shown in Figure 2.

Table 1: Moments, Skewness and Kurtosis of NUMW Distribution

Measure	P_1	P_2	P_3	P_4
μ'_1	0.2734	0.5191	0.6751	0.9773
μ'_2	0.0832	0.2852	0.5755	0.9555
μ'_3	0.0295	0.1660	0.5271	0.9346
μ'_4	0.0126	0.1022	0.4974	0.9144
$\mu_2 = \sigma^2$	0.0085	0.0158	0.1197	0.0004
μ_3	0.0021	0.0016	-0.0231	-8.38×10^{-6}
μ_4	0.0009	0.0008	0.0247	5.73×10^{-7}
CS	2.6552	0.8043	-0.5586	-1.1186
CK	13.0921	3.3430	1.7207	3.9097

The rth incomplete moment of the NUMW distribution is also obtained as a solution to the equation

$$m_r(t) = \sum_{i=0}^{\infty} \Delta_{kl} \varphi^i \vartheta(i\rho + k + l) \int_0^t w^r (1-w)^{\vartheta(i\rho+k+l)-1} dw. \tag{30}$$

The solution to equation (30) is given as

$$m_r(t) = \sum_{i=0}^{\infty} \Delta_{kl} \varphi^i \vartheta(i\rho + k + l) \mathbb{B}\left(t; r+1, \vartheta(i\rho+k+l)\right),\ \ r = 1,2,3,\ldots, \tag{31}$$

where $\mathbb{B}(t;a,b) = \int_0^t w^{a-1}(1-w)^{b-1}dw$ is the incomplete beta function.

© 2026 NSP
Natural Sciences Publishing Cor.

3.2.2 Moment Generating Function

The moment generating function (mgf) of a distribution is defined as

$$M_W(t) = \mathbb{E}\left[e^{tW}\right] = \sum_{s=0}^{\infty} \frac{t^s}{s!}\mu_s',$$

where μ_s' is the sth ordinary moment of the distribution. Substituting equation (28) into the definition gives the mgf as

$$M_W(t) = \sum_{s=0}^{\infty} \frac{t^s}{s!}\mu_s' = \sum_{s=0}^{\infty}\sum_{i=0}^{\infty} \frac{t^s}{s!}\Delta_{kl}\varphi^i \vartheta(i\rho+k+l)\mathbb{B}\left(s+1, \vartheta(i\rho+k+l)\right). \tag{32}$$

3.3 Stochastic Ordering

Stochastic ordering is an important concept in quantifying uncertainty. It is used to quantify the concept of one random variable being greater or less than another random variable. In risk analysis, stochastic ordering can be used to determine if one variable is likely to have greater outcomes or risk than another variable. It also has uses in performance comparison, reliability theory, among others.

Let W_1 and W_2 be NUMW random variables with PDFs $f(w;\varphi_1,\rho,\varsigma,\vartheta)$ and $f(w;\varphi_2,\rho,\varsigma,\vartheta)$. Also, letting $\varphi_1 > \varphi_2$, then we can show that $W_1 \geq W_2$ in likelihood ratio order ($W_1 \geq_{lr} W_2$). To achieve this, the ratio of the PDFs is examined. The ratio is obtained as

$$\frac{f(w;\varphi_2,\rho,\varsigma,\vartheta)}{f(w;\varphi_1,\rho,\varsigma,\vartheta)} = \left(\frac{\varphi_2}{\varphi_1}\right)\exp\left(-(\varphi_2-\varphi_1)(-\ln u)^{\rho}u^{-\varsigma}\right).$$

To further examine the nature of the ratio, the log of the ratio is obtained as

$$\ln\frac{f(w;\varphi_2,\rho,\varsigma,\vartheta)}{f(w;\varphi_1,\rho,\varsigma,\vartheta)} = \ln\left(\frac{\varphi_2}{\varphi_1}\right) - (\varphi_2-\varphi_1)(-\ln u)^{\rho}u^{-\varsigma}. \tag{33}$$

Differentiating equation (33) gives

$$\frac{d}{dw}\ln\frac{f(w;\varphi_2,\rho,\varsigma,\vartheta)}{f(w;\varphi_1,\rho,\varsigma,\vartheta)} = (\varphi_2-\varphi_1)\frac{\vartheta(1-w)^{\vartheta-1}\left(\rho+\ln u^{-\varsigma}\right)}{(-\ln u)^{1-\rho}u^{\varsigma+1}}. \tag{34}$$

From equation (34), it can be noted that for $\varphi_1 > \varphi_2$, then $\frac{d}{dw}\ln\frac{f(w;\varphi_2,\rho,\varsigma,\vartheta)}{f(w;\varphi_1,\rho,\varsigma,\vartheta)} < 0$. This implies that the ratio $\frac{f(w;\varphi_2,\rho,\varsigma,\vartheta)}{f(w;\varphi_1,\rho,\varsigma,\vartheta)}$ is a decreasing function of w. Thus, $W_1 \geq_{lr} W_2$.

To further support the assertion, graphical results are shown in Figure 3 for fixed values $\rho = 0.2$, $\varsigma = 0.1$ and $\vartheta = 0.2$. It can be observed that when $\varphi_1 > \varphi_2$, then decreasing shapes can be observed, while increasing shapes are observed for $\varphi_1 < \varphi_2$.

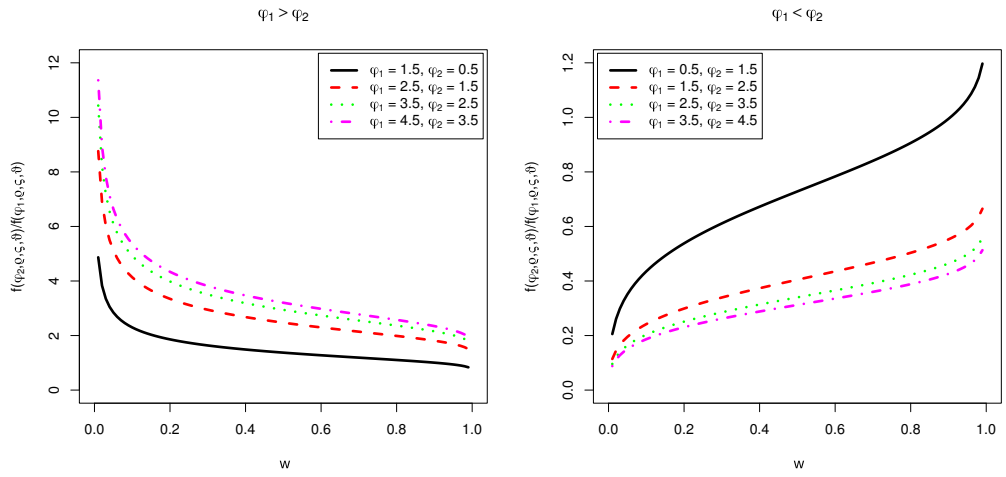


Fig. 3: PDF Ratio Plots of NUMW Distribution

© 2026 NSP
Natural Sciences Publishing Cor.

3.4 Order Statistics

Let $\{w_i\}_{i=1}^n$ be a random sample of size n generated from the NUMW distribution. The corresponding order statistics of the sample are given as $\{w_{i:n}\}_{i=1}^n$. The CDF of the rth ordered statistic of the n ordered sample of the NUMW distribution is given as

$$F_{r:n}(w) = \sum_{j=r}^{n} \binom{n}{j} [F(w)]^j [1-F(w)]^{n-j}.$$

Using binomial expansion, the CDF can be written as

$$F_{r:n}(w) = \sum_{j=r}^{n} \sum_{p=0}^{n-j} \binom{n}{j} \binom{n-j}{p} (-1)^p [F(w)]^{j+p}. \tag{35}$$

Substituting equation (7) into equation (35) gives the CDF of the rth order statistic as

$$F_{r:n}(w) = \sum_{j=r}^{n} \sum_{p=0}^{n-j} \binom{n}{j} \binom{n-j}{p} (-1)^p \exp\left(-\varphi(j+p)(-\ln u)^{\rho} u^{-\varsigma}\right).$$

The CDF of the first and last order statistic of the NUMW distribution are defined, respectively, as

$$F_{1:n}(w) = 1-[1-F(w)]^n = 1-\sum_{i=0}^{n} \binom{n}{i} (-1)^i [F(w)]^i$$

and

$$F_{n:n}(w) = [F(w)]^n.$$

Again, substituting equation (7) into the definitions gives the first and last order statistic of the NUMW distribution, respectively, as

$$F_{1:n}(w) = 1-\sum_{i=0}^{n} \binom{n}{i} (-1)^i \exp\left(-\varphi i(-\ln u)^{\rho} u^{-\varsigma}\right)$$

and

$$F_{n:n}(w) = \exp\left(-\varphi n(-\ln u)^{\rho} u^{-\varsigma}\right).$$

The plots of the expected minimum and maximum (min-max) of the order statistics are presented in Figure 4 to show the various degrees of asymmetry that can be assumed by the NUMW distribution. For certain parameter values, the plots are obtained using $\mathbb{E}[W_{1:n}]$ and $\mathbb{E}[W_{n:n}]$. As observed, the distribution can assume various shapes, including positive skewness, negative skewness and approximately symmetric.

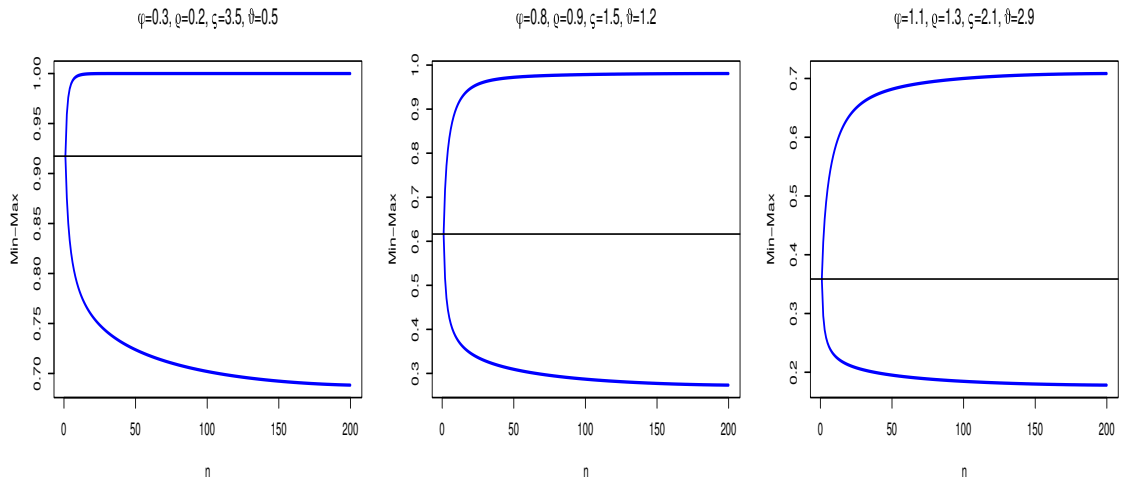


Fig. 4: Min-Max Plots of NUMW Distribution

© 2026 NSP
Natural Sciences Publishing Cor.

3.5 Lorenz and Bonferroni Curves

For measures of inequality in a population, Lorenz curve (LZC) and Bonferroni curve (BFC) are often used. LZC and BFC are obtained for the NUMW distribution. The following formulas are used to obtain LZC and BFC, respectively, as

$$LZC(w) = \frac{m_1(w)}{\mu} \tag{36}$$

and

$$BFC(w) = \frac{m_1(w)}{\mu F(w)}, \tag{37}$$

where μ is the mean, $m_1(w)$ is the first incomplete moment and $F(w)$ is the CDF of the NUMW distribution. For $r = 1$, equation (31) gives the first incomplete moment of the NUMW distribution. Substituting that into the formulas give the LZC and BFC for the NUMW distribution as

$$LZC(w) = \frac{\vartheta}{\mu}\sum_{i=0}^{\infty}\Delta_{kl}\varphi^i(i\rho+k+l)\mathbb{B}(w;2,\vartheta(i\rho+k+l)) \tag{38}$$

and

$$BFC(w) = \frac{\vartheta}{\mu F(w)}\sum_{i=0}^{\infty}\Delta_{kl}\varphi^i(i\rho+k+l)\mathbb{B}(w;2,\vartheta(i\rho+k+l)). \tag{39}$$

The LZC and BFC can also be obtained, respectively, attributed to [41], using

$$LZC(\tau) = \frac{1}{\mu}\int_0^{\tau} Q_W(x)dx \tag{40}$$

and

$$BFC(\tau) = \frac{1}{\mu\tau}\int_0^{\tau} Q_W(x)dx, \tag{41}$$

where $\tau \in (0,1)$ and $Q_W(\cdot)$ is the QF of the NUMW distribution. Figure 5 depicts the LZC and BFC for the NUMW distribution. In the LZC plot, the 45 degree line shows the point of equality. The greater the distance between the curve and the diagonal, the higher the inequality.

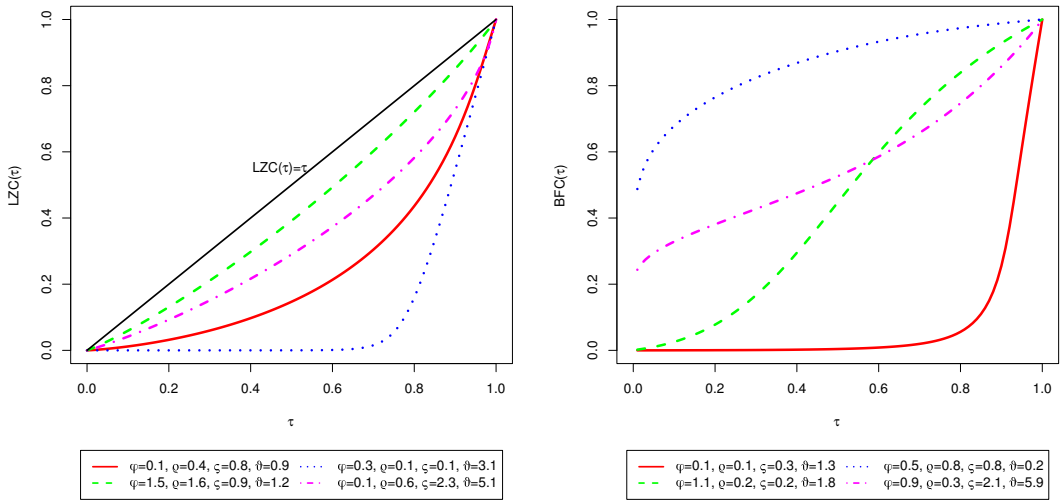


Fig. 5: LZC (Left) and BFC (Right) Plots of NUMW Distribution

© 2026 NSP
Natural Sciences Publishing Cor.

4 Estimation of Model Parameters

This section presents the parameter estimation of the NUMW distribution using maximum likelihood (ML) method.

4.1 Maximum Likelihood Estimation

To proceed with the presentation, let $\{w_i\}_{i=1}^n$ be n random samples drawn from the NUMW distribution and $\Theta = (\varphi, \rho, \varsigma, \vartheta)'$ be the vector of unknown parameters of the distribution. The joint PDF of the sample is obtained as

$$\mathscr{L}(\Theta) = \prod_{i=1}^{n} f(w_i;\Theta).$$

The ML procedure results in the set of parameter values that maximize the joint PDF. However, for ease of optimization, the log of the joint PDF is obtained as the log-likelihood (LL) function as

$$\ell(\Theta) = \sum_{i=1}^{n} \ln f(w_i;\Theta).$$

Substituting equation (8) into the LL function gives

$$\begin{aligned}\ell(\Theta) =& n\ln(\varphi\vartheta) + (\vartheta-1)\sum_{i=1}^{n}\ln(1-w_i) + \sum_{i=1}^{n}\ln\left(\rho + \ln u_i^{-\varsigma}\right) - \varphi\sum_{i=1}^{n}(-\ln u_i)^{\rho}u_i^{-\varsigma} \\ & -(\varsigma+1)\sum_{i=1}^{n}\ln u_i + (\rho-1)\sum_{i=1}^{n}\ln(-\ln u_i),\end{aligned} \tag{42}$$

where $u_i = 1-(1-w_i)^{\vartheta}$. The partial derivatives of equation (42) with respect to each parameter gives the score functions as

$$\frac{\partial\ell}{\partial\varphi} = \frac{n}{\varphi} - \sum_{i=1}^{n}[-\ln u_i]^{\rho}u_i^{-\varsigma}, \tag{43}$$

$$\frac{\partial\ell}{\partial\rho} = \sum_{i=1}^{n}\frac{1}{\rho-\varsigma\ln u_i} + \sum_{i=1}^{n}\ln(-\ln u_i) - \varphi\sum_{i=1}^{n}\frac{[-\ln u_i]^{\rho}\ln(-\ln u_i)}{u_i^{\varsigma}}, \tag{44}$$

$$\frac{\partial\ell}{\partial\varsigma} = \sum_{i=1}^{n}\frac{-\ln u_i}{\rho-\varsigma\ln u_i} - \sum_{i=1}^{n}\ln u_i + \varphi\sum_{i=1}^{n}\frac{[-\ln u_i]^{\rho}\ln u_i}{u_i^{\varsigma}} \tag{45}$$

and

$$\begin{aligned}\frac{\partial\ell}{\partial\vartheta} =& \frac{n}{\vartheta} + \sum_{i=1}^{n}\ln(1-w_i) + \sum_{i=1}^{n}\frac{(1-w_i)^{\vartheta}\ln(1-w_i)}{u_i}\left[\frac{\varsigma}{\rho-\varsigma\ln u_i} + (\varsigma+1) + \frac{1-\rho}{\ln u_i}\right] \\ & -\varphi\sum_{i=1}^{n}\frac{(1-w_i)^{\vartheta}\ln(1-w_i)[-\ln u_i]^{\rho-1}}{u_i^{\varsigma+1}}[\rho-\varsigma\ln u_i].\end{aligned} \tag{46}$$

Ideally, setting the score functions to zero and solving simultaneously gives the estimators. However, the intricacies of the score functions present a challenging situation as they have no closed-form solution. Hence, numerical maximization is used to obtain the point estimates. R statistical software [42], version 4.5.2, is used in this study to estimate the parameters of the distribution. Specifically, the *stats* package within the software via *nlminb* routine is used.

For interval estimation, confidence intervals (CIs) for the parameters can be obtained from the large sample behaviour of the ML estimator $\hat{\Theta}$. Under the usual regularity conditions, $\sqrt{n}(\hat{\Theta}-\Theta) \xrightarrow{d} \mathscr{N}_4\left(\mathbf{0}, \mathscr{I}(\Theta)^{-1}\right)$, where $\mathscr{I}(\Theta)$ is the Fisher information matrix (IM) per observation. Since $\mathscr{I}(\Theta)$ depends on the unknown parameters and is difficult to obtain in closed form, it is estimated by $n^{-1}\mathscr{J}_{obs}(\Theta)$, where $\mathscr{J}_{obs}(\Theta)$ is the observed IM. Writing $\ell = \ell(\Theta)$ for the LL, the observed

© 2026 NSP
Natural Sciences Publishing Cor.

IM is the negative Hessian of ℓ, defined as

$$\mathscr{J}_{obs}(\Theta) = -\frac{\partial^2 \ell(\boldsymbol{\Theta})}{\partial \boldsymbol{\Theta}\, \partial \boldsymbol{\Theta}^{\top}} = -\begin{pmatrix} \frac{\partial^2 \ell}{\partial \varphi^2} & \frac{\partial^2 \ell}{\partial \varphi\, \partial \rho} & \frac{\partial^2 \ell}{\partial \varphi\, \partial \varsigma} & \frac{\partial^2 \ell}{\partial \varphi\, \partial \vartheta} \\ \frac{\partial^2 \ell}{\partial \rho\, \partial \varphi} & \frac{\partial^2 \ell}{\partial \rho^2} & \frac{\partial^2 \ell}{\partial \rho\, \partial \varsigma} & \frac{\partial^2 \ell}{\partial \rho\, \partial \vartheta} \\ \frac{\partial^2 \ell}{\partial \varsigma\, \partial \varphi} & \frac{\partial^2 \ell}{\partial \varsigma\, \partial \rho} & \frac{\partial^2 \ell}{\partial \varsigma^2} & \frac{\partial^2 \ell}{\partial \varsigma\, \partial \vartheta} \\ \frac{\partial^2 \ell}{\partial \vartheta\, \partial \varphi} & \frac{\partial^2 \ell}{\partial \vartheta\, \partial \rho} & \frac{\partial^2 \ell}{\partial \vartheta\, \partial \varsigma} & \frac{\partial^2 \ell}{\partial \vartheta^2} \end{pmatrix},$$

evaluated at $\Theta = \hat{\Theta}$. For large n, $\hat{\Theta}$ follows the Gaussian distribution with mean Θ and variance-covariance matrix $\mathscr{J}_{obs}(\hat{\Theta})^{-1}$. Let $\text{se}(\hat{\theta}_j) = \sqrt{\left[\mathscr{J}_{obs}(\hat{\Theta})^{-1}\right]_{jj}}$ denote the estimated standard error of $\hat{\theta}_j$. An approximate $100(1-q)\%$ CI for the j-th component θ_j of Θ is (L_j, U_j), with lower and upper limits defined as $L_j = \hat{\theta}_j - z_{q/2}\,\text{se}(\hat{\theta}_j)$ and $U_j = \hat{\theta}_j + z_{q/2}\,\text{se}(\hat{\theta}_j)$, where $z_{q/2}$ is the upper $q/2$ point of the standard Gaussian distribution.

4.2 Simulation Studies

The estimators of the parameters are examined via Monte Carlo simulation studies to assess their accuracy and performance. The following algorithm was used for the simulation studies:

Algorithm 1: Simulation Studies for NUMW Distribution

Input: $k = 8$ (length of sample size vector $n = 30, 50, 100, 200, 350, 600, 800$ and 1000)).
Input: Specify the true values of the parameters: Θ.
Input: $N = 1000$ (Number of iterations).

for $i = 1$ **to** k **do**
  for $j = 1$ **to** N **do**
    Generate n NUMW distributed random numbers using its quantile function $Q_W(\tau)$, where $\tau \sim \text{Uniform}(0,1)$.
    Estimate the parameters of the distribution.
  Compute the average estimate (AE), absolute bias (AB), root mean square error (RMSE), average coverage probabilities (CP) and average lengths (AL) of the asymptotic confidence intervals using the following formulas, respectively:

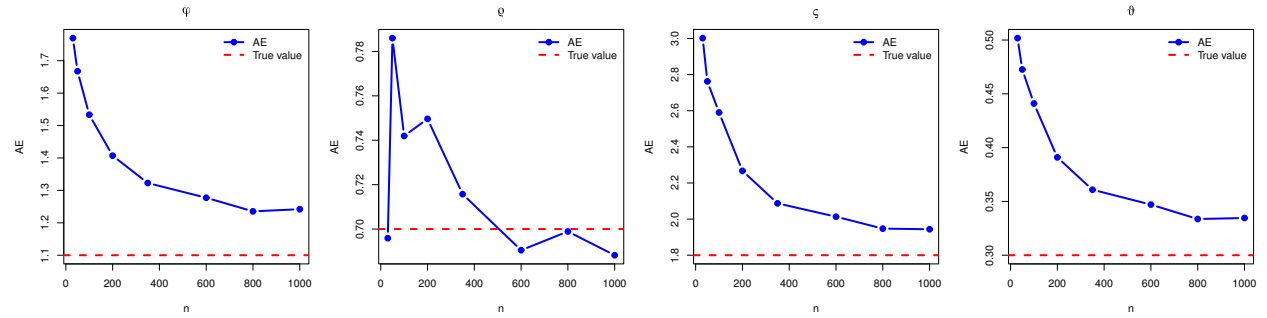
$$\text{AE} = \frac{1}{N}\sum_{j=1}^{N}\hat{\Theta}_j, \quad \text{AB} = \frac{1}{N}\sum_{j=1}^{N}\left|\hat{\Theta}_j - \Theta_j\right|, \quad \text{RMSE} = \sqrt{\frac{1}{N}\sum_{j=1}^{N}\left(\hat{\Theta}_j - \Theta_j\right)^2},$$

$$\text{CP} = \frac{1}{N}\sum_{j=1}^{N}\mathbb{I}(L_j \le \Theta_j \le U_j) \quad \text{and} \quad \text{AL} = \frac{1}{N}\sum_{j=1}^{N}(U_j - L_j),$$

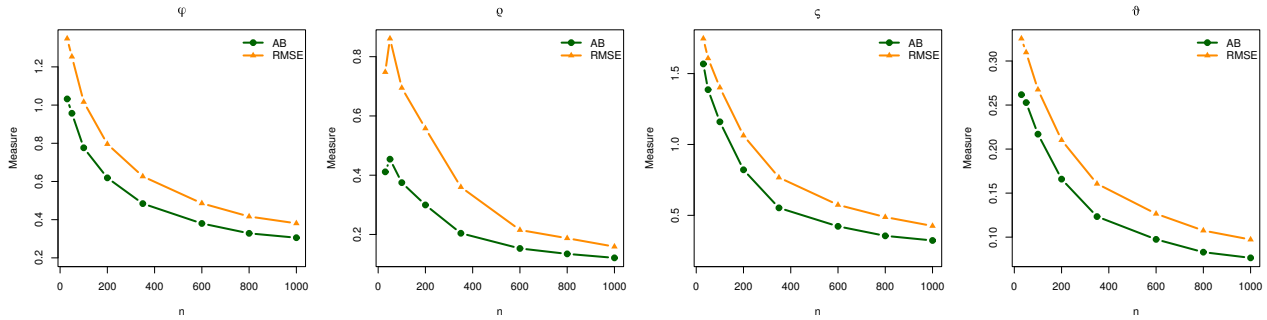
  where U_j and L_j are the upper and lower confidence limits in the jth replication, respectively, and $\mathbb{I}(\cdot)$ is an indicator function.

Algorithm 1 is replicated for three combinations of the parameter values. These include $\boldsymbol{I} = (\varphi = 1.1, \rho = 0.7, \varsigma = 1.8, \vartheta = 0.3)$, $\boldsymbol{II} = (\varphi = 0.4, \rho = 0.2, \varsigma = 0.6, \vartheta = 0.7)$ and $\boldsymbol{III} = (\varphi = 0.2, \rho = 1.2, \varsigma = 1.1, \vartheta = 0.3)$. The results are presented in Figures 6, 7 and 8. The true parameter values are marked by a horizontal line in the plots of AE in Figures 6, 7 and 8. From the figures, the AEs approach their respective true values, while the AB and RMSE decrease towards zero as n increases. This indicates that the estimators are consistent, although convergence is slow for some parameters, notably φ and ϑ. Alos, the CPs generally move towards the nominal 95% level as n increases, although they remain below it for some parameters even at $n = 1000$. Overall, the ML estimators perform satisfactorily for moderate to large samples, making them suitable for estimating the parameters of the NUMW distribution in practice.

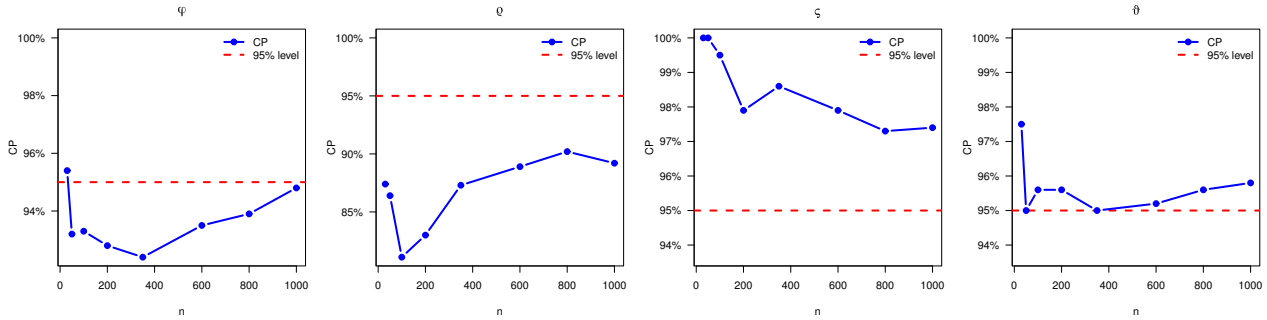
© 2026 NSP
Natural Sciences Publishing Cor.



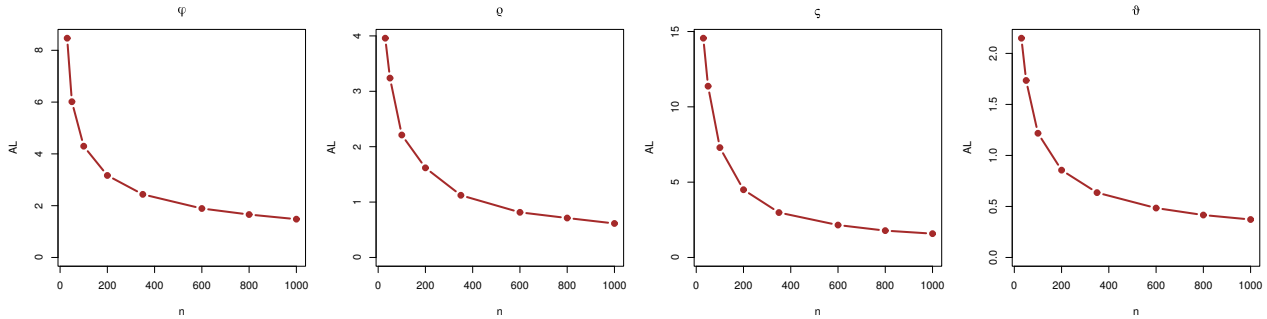
(a) AE



(b) AB and RMSE



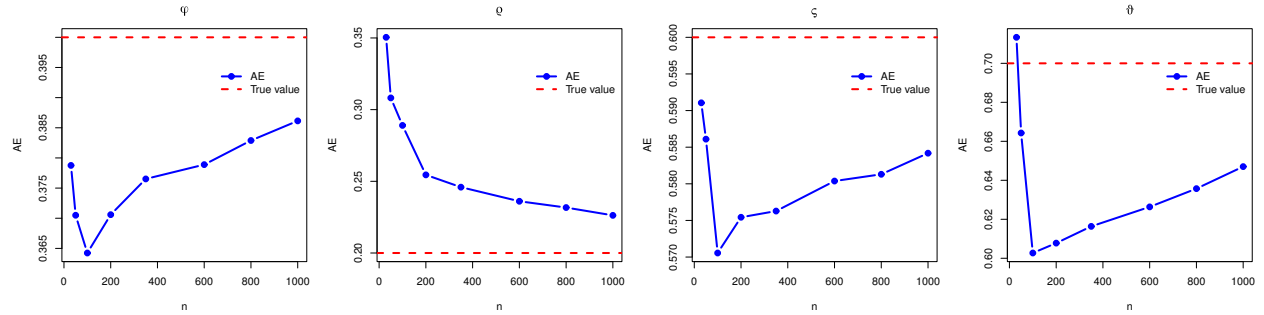
(c) CP



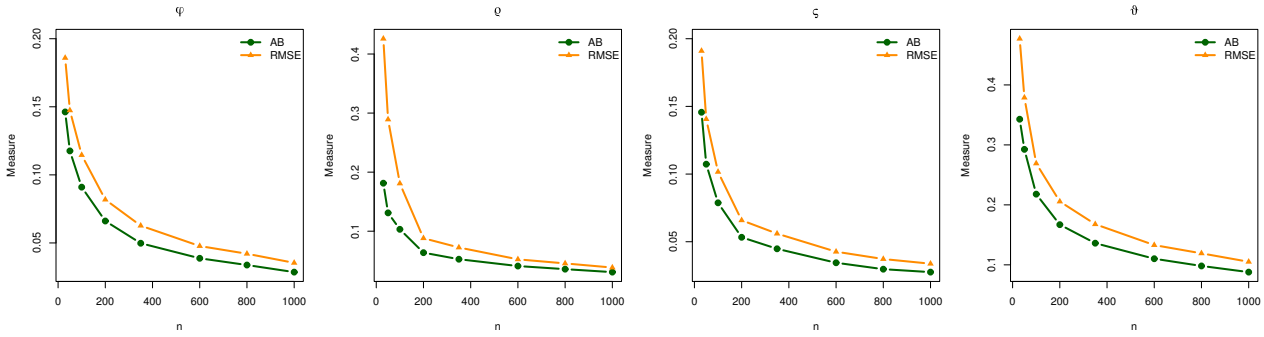
(d) AL

Fig. 6: Simulation Results for Scenario ***I***

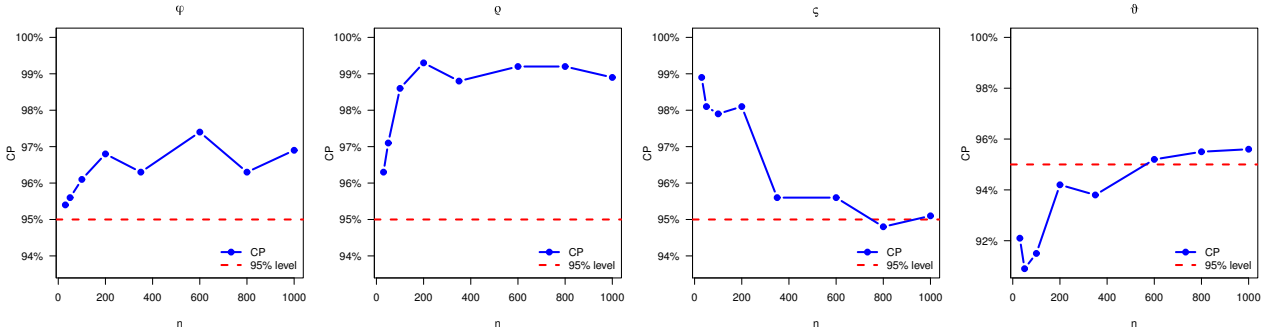
© 2026 NSP
Natural Sciences Publishing Cor.



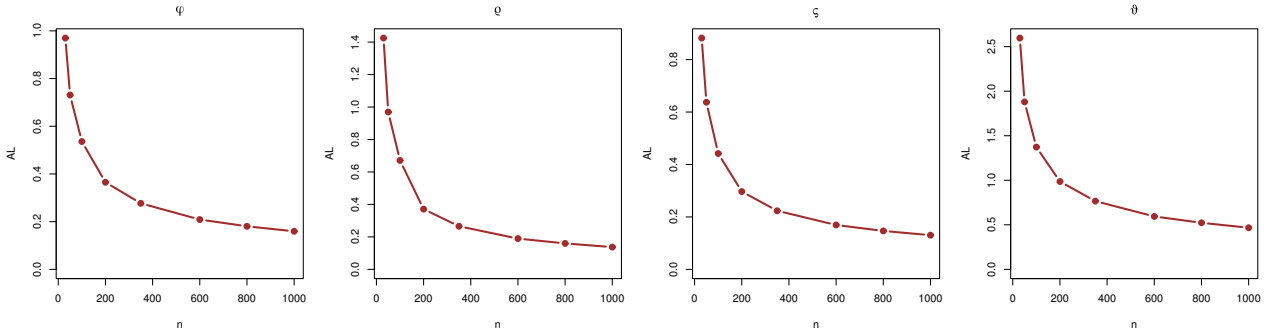
(a) AE



(b) AB and RMSE



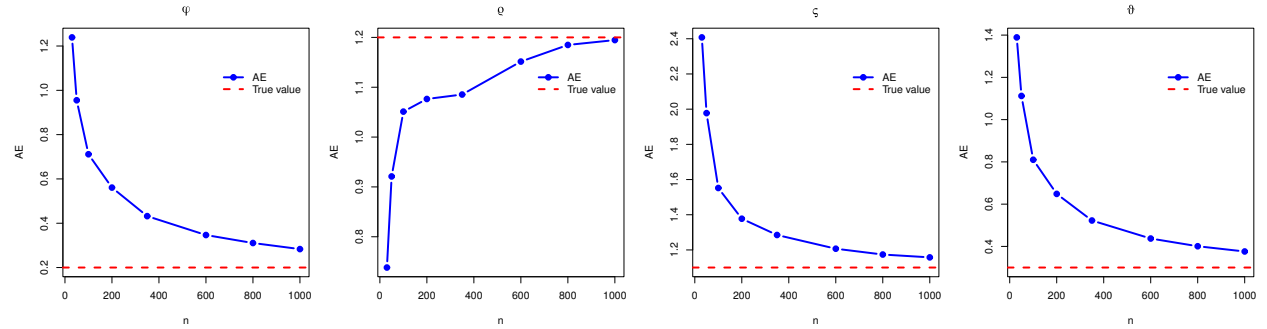
(c) CP



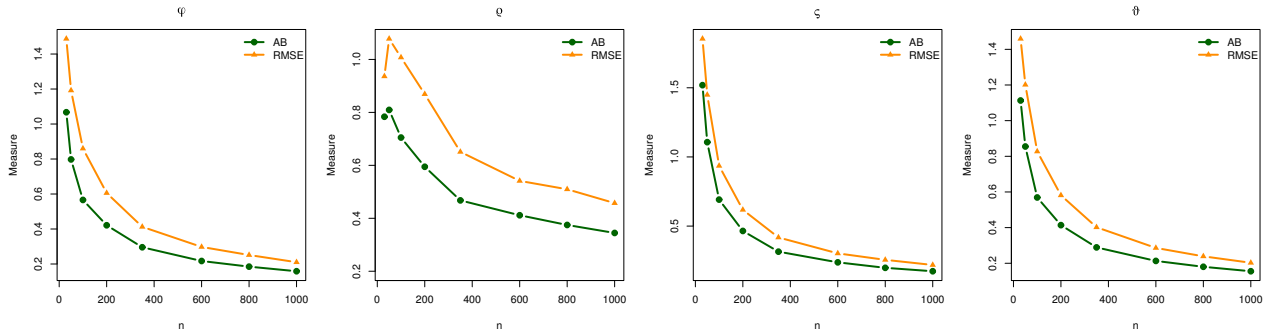
(d) AL

Fig. 7: Simulation Results for Scenario ***II***

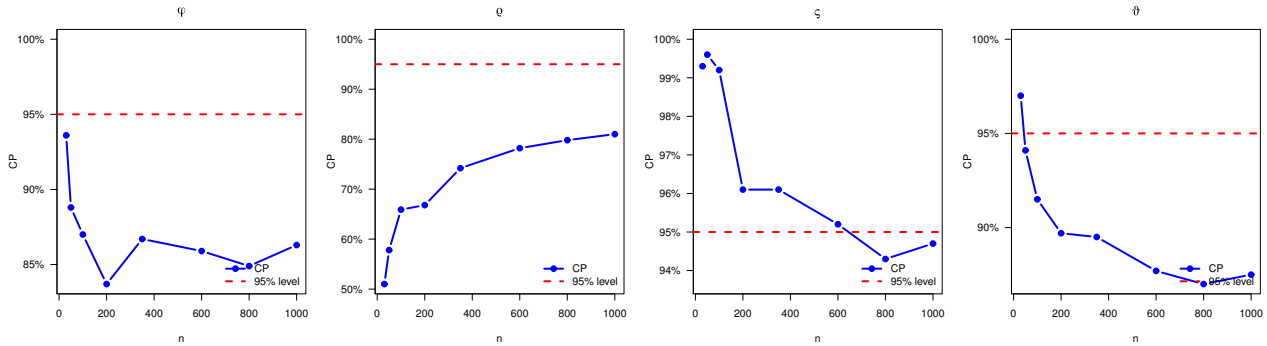
© 2026 NSP
Natural Sciences Publishing Cor.



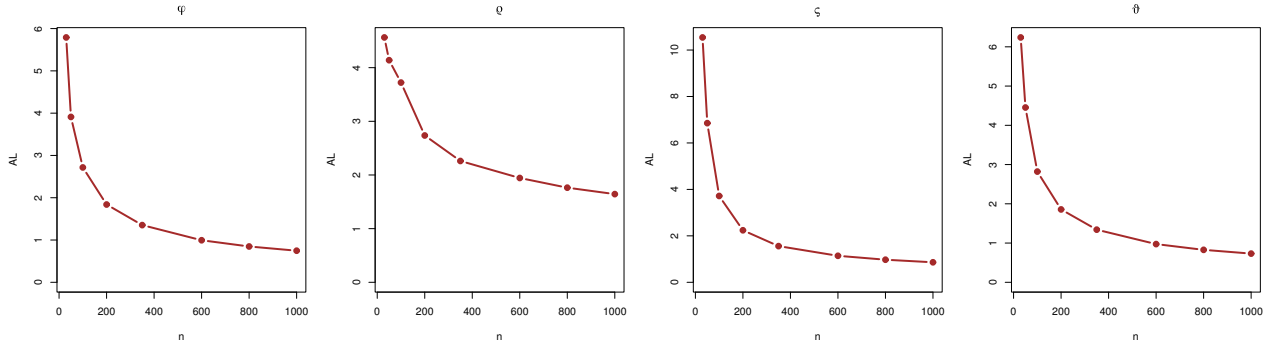
(a) AE



(b) AB and RMSE



(c) CP



(d) AL

Fig. 8: Simulation Results for Scenario ***III***

© 2026 NSP
Natural Sciences Publishing Cor.

5 Quantile Regression Model

This section presents QR model for the NUMW distribution, denoted NUMWQR. To obtain the model, let $\eta = Q_W(\tau),\ \eta \in (0,1)$ in the QF of the NUMW distribution in equation (25). Thus η is the quantile parameter. Making φ the subject in the QF gives

$$\varphi = -\frac{\ln(\tau)}{[-\ln(1-(1-\eta)^{\vartheta})]^{\rho}\,[1-(1-\eta)^{\vartheta}]^{-\varsigma}},\quad \eta \in (0,1), \tau \in (0,1). \tag{47}$$

Substituting equation (47) into the PDF of the NUMW distribution in equation (8) gives a re-parameterized PDF of the NUMW distribution as

$$f(w) = \frac{\vartheta(1-w)^{\vartheta-1}(\varsigma \ln u - \rho)}{u(-\ln u)} Pe^{P},\quad w \in (0,1), \tag{48}$$

where $\eta \in (0,1), \tau \in (0,1), \rho > 0, \vartheta > 0, \varsigma > 0$ and $P = \left(\frac{\ln u}{\ln\left(1-(1-\eta)^{\vartheta}\right)}\right)^{\rho}\left(\frac{1-(1-\eta)^{\vartheta}}{u}\right)^{\varsigma}\ln(\tau)$.

In order to incorporate covariates into the regression model, the following structure is used:

$$g(\eta_h) = x_h'\boldsymbol{\delta},\quad h = 1,2,3,\ldots,n, \tag{49}$$

where $g(\cdot)$ is a link function, η_h is the hth quantile parameter, x_h' is the hth covariate vector and $\boldsymbol{\delta} = (\delta_0, \delta_1, \ldots, \delta_d)'$ is the unknown parameter vector. Various link functions are available for connecting the quantile to the covariates. In this study, the logit link function is used. It is used because the quantile of the NUMW distribution is defined on the unit interval and for easy interpretability of results. The function is defined as

$$\ln\left(\frac{\eta_h}{1-\eta_h}\right) = x_h'\boldsymbol{\delta},\quad h = 1,2,3,\ldots,n.$$

Making η_h the subject and substituting into the reparameterized PDF in equation (48) gives PDF of the regression model.

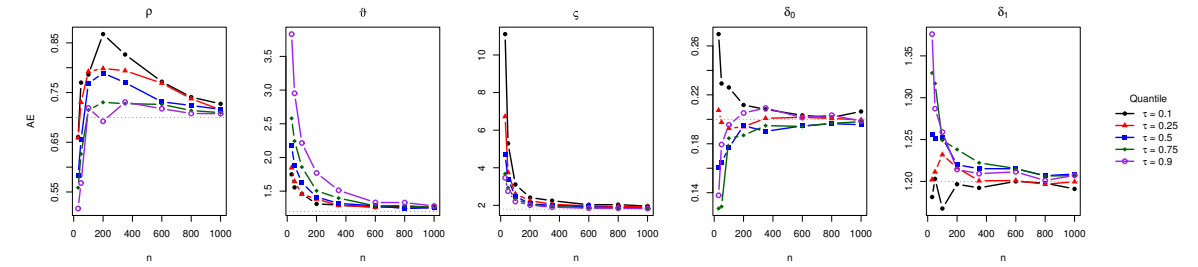
Let $\Psi = (\rho, \vartheta, \varsigma, \delta_0, \delta_1, \ldots, \delta_d)'$ be the parameter vector of NUMWQR model. The ML estimators of the parameters can be obtained by optimizing the following log-likelihood function:

$$\begin{aligned}\ell(\Psi) =& n\ln(\vartheta) + (\vartheta-1)\sum_{h=1}^{n}\ln(1-w_h) + \sum_{h=1}^{n}\ln(\rho - \varsigma\ln u_h)\\ &- \sum_{h=1}^{n}\ln u_h - \sum_{h=1}^{n}\ln(-\ln u_h)\\ &+ \sum_{h=1}^{n}\left[\rho\ln\left(\frac{\ln u_h}{\ln[1-(1-\eta_h)^{\vartheta}]}\right) + \varsigma\ln\left(\frac{1-(1-\eta_h)^{\vartheta}}{u_h}\right) + \ln(-\ln\tau)\right]\\ &+ \ln(\tau)\sum_{h=1}^{n}\left[\left(\frac{\ln u_h}{\ln[1-(1-\eta_h)^{\vartheta}]}\right)^{\rho}\left(\frac{1-(1-\eta_h)^{\vartheta}}{u_h}\right)^{\varsigma}\right],\end{aligned}$$

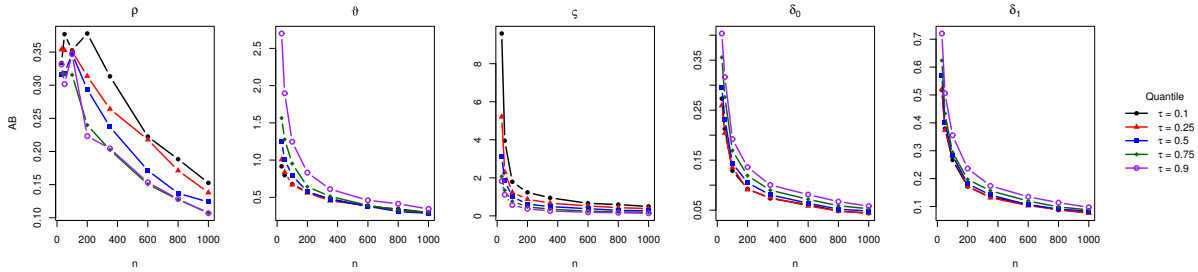
where $u_h = 1-(1-w_h)^{\vartheta}$, $\eta_h = \frac{e^{x_h'\boldsymbol{\delta}}}{1+e^{x_h'\boldsymbol{\delta}}}$, $h = 1,2,3,\ldots,n$. Numerical methods are employed to obtain the estimates of the parameters of the model via R statistical software [42].

To verify whether fitted QR models are suitable, residual analysis is employed. Cox-Snell residuals (CSR) [43] are used to assess fitted QR models in this study. CSR is defined as $\hat{r}_i = -\ln\left[1-F(w_i;\hat{\Theta})\right],\ i = 1,2,3,\ldots,n$ where $F(w_i;\hat{\Theta})$ is the re-parameterized CDF. If the model is adequate, CSR should be standard exponentially distributed.

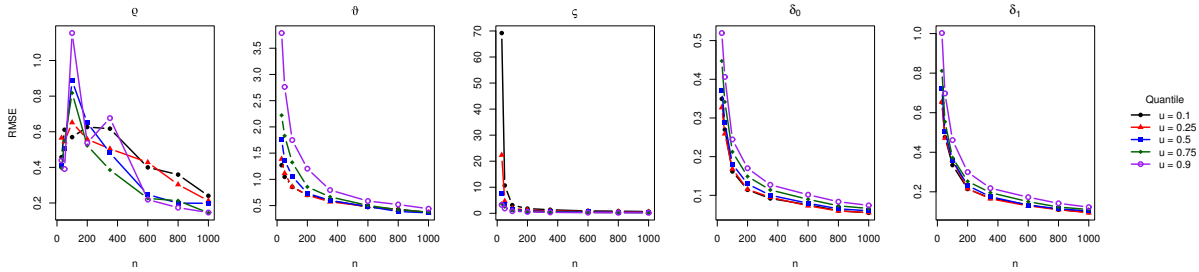
© 2026 NSP
Natural Sciences Publishing Cor.



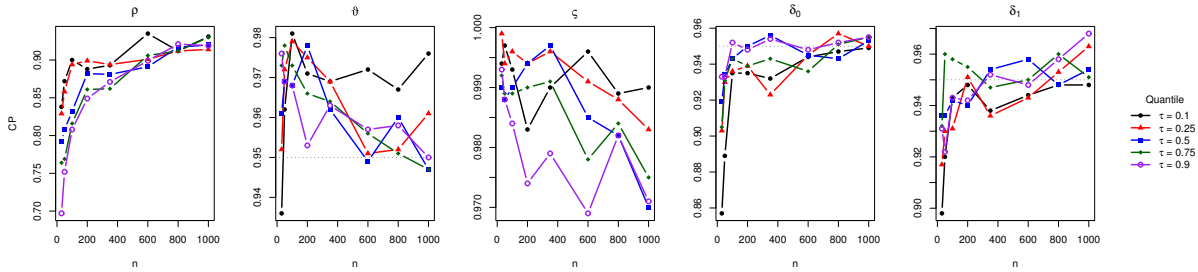
(a) AE



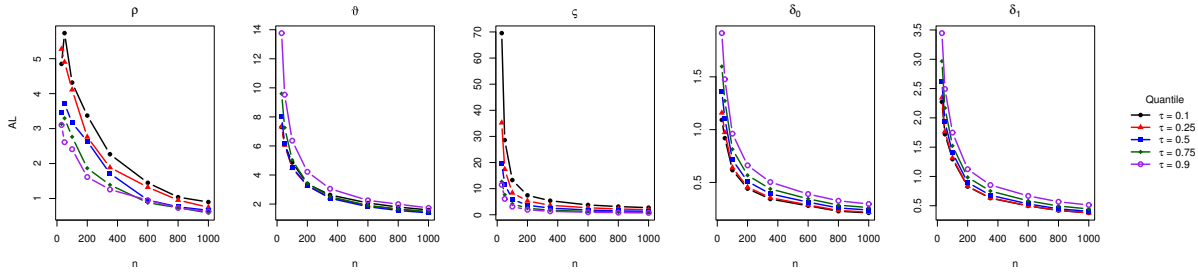
(b) AB



(c) RMSE



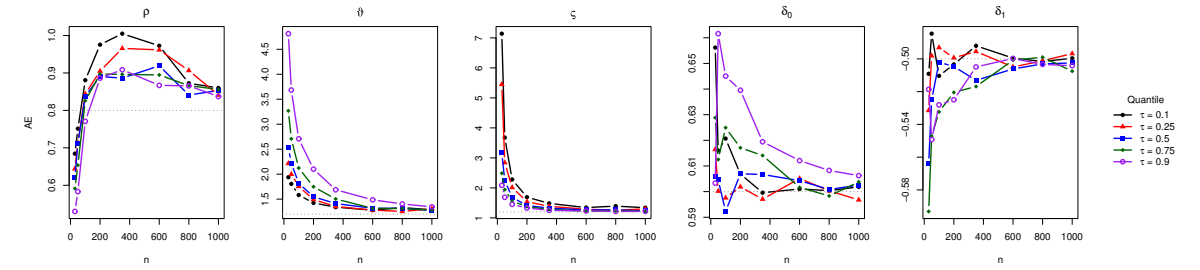
(d) CP



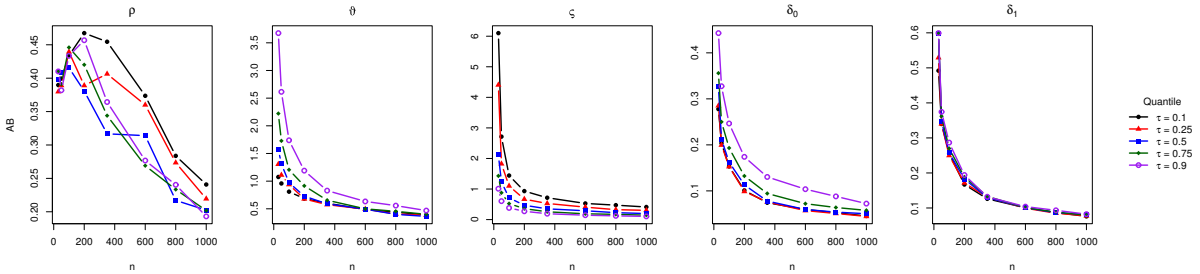
(e) AL

Fig. 9: Regression: Simulation Results for Parameter Set $\boldsymbol{R_1}$

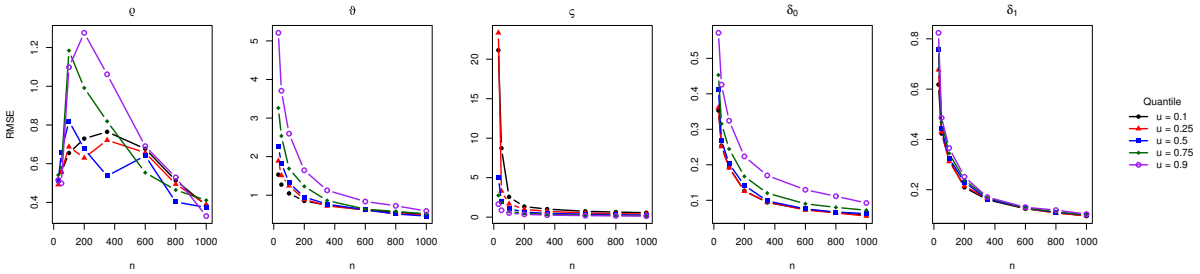
© 2026 NSP
Natural Sciences Publishing Cor.



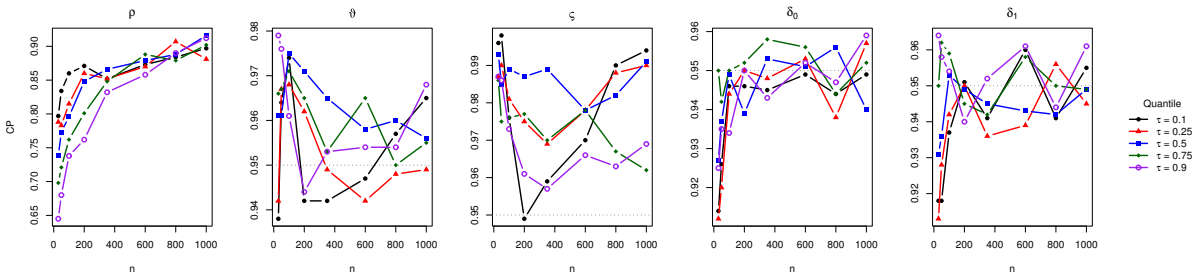
(a) AE



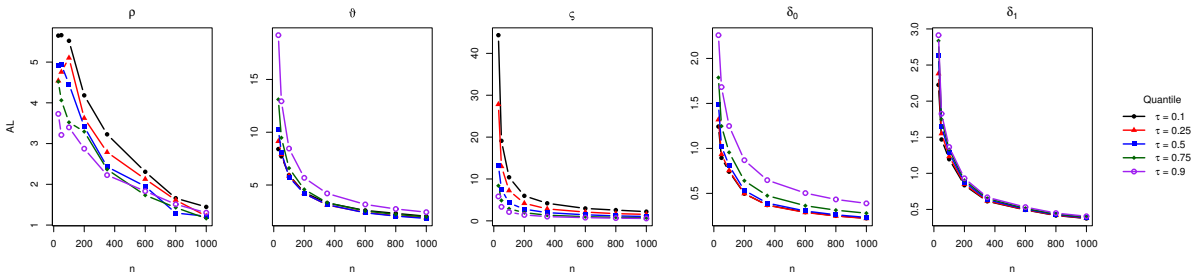
(b) AB



(c) RMSE



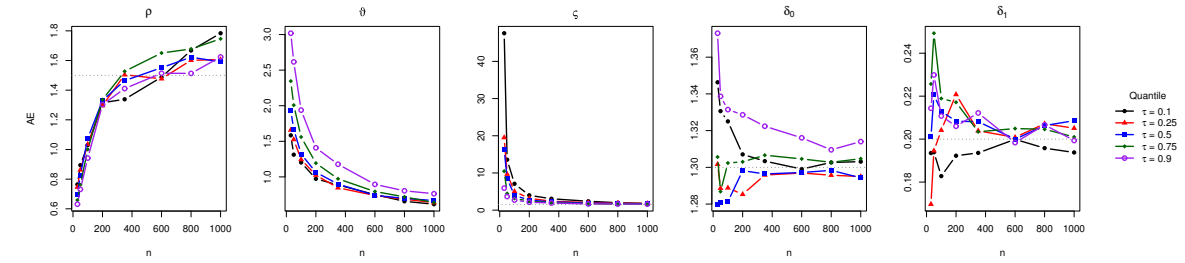
(d) CP



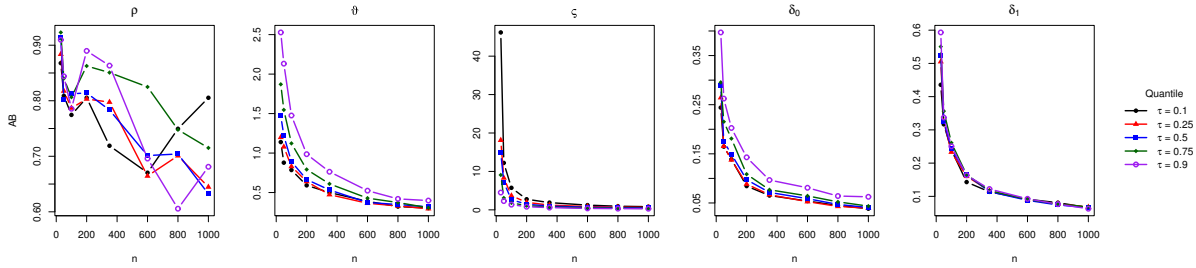
(e) AL

Fig. 10: Regression: Simulation Results for Parameter Set $\boldsymbol{R_2}$

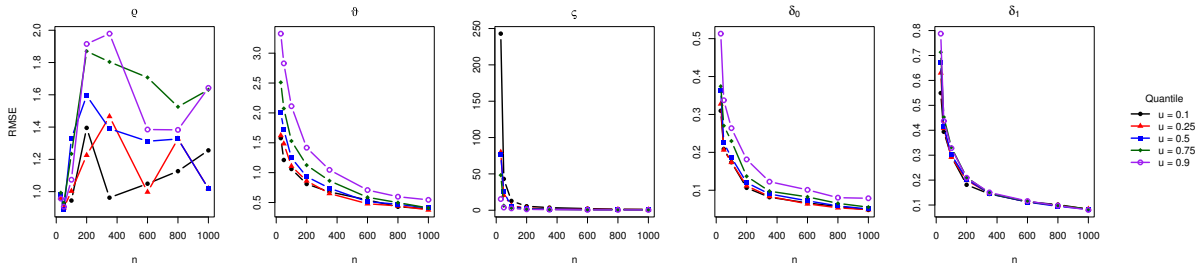
© 2026 NSP
Natural Sciences Publishing Cor.



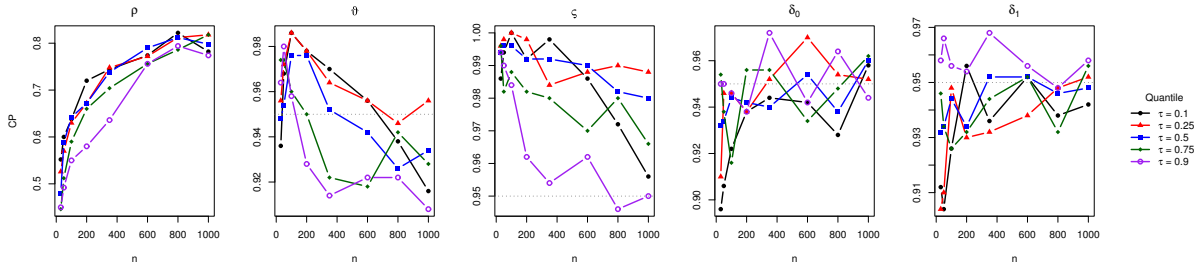
(a) AE



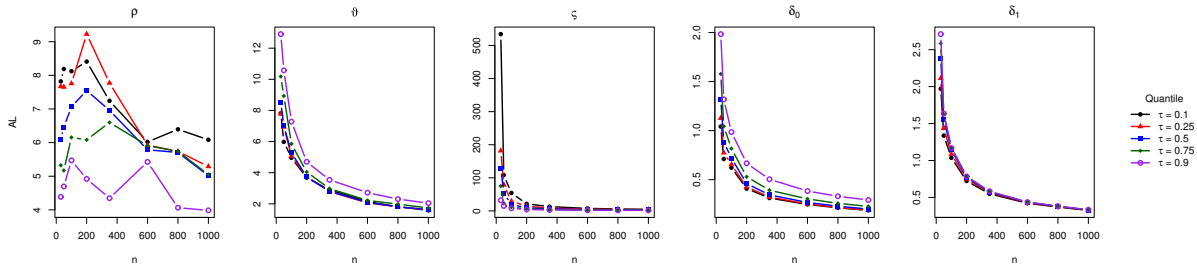
(b) AB



(c) RMSE



(d) CP



(e) AL

Fig. 11: Regression: Simulation Results for Parameter Set $\boldsymbol{R_3}$

© 2026 NSP
Natural Sciences Publishing Cor.

5.1 Simulation Studies

The ML estimators of NUMWQR model are assessed via Monte Carlo simulation. The following regression structure is used for the simulation studies:

$$\eta_h = \frac{e^{\delta_0+\delta_1 x_h}}{1+e^{\delta_0+\delta_1 x_h}}, \quad h = 1,2,3,\ldots,n.$$

Algorithm 2 presents the algorithm for the simulation studies.

Algorithm 2: Simulation Studies for NUMWQR Model

Input: $k = 8$ (length of sample size vector $n = 30, 50, 100, 200, 350, 600, 800$ and 1000)).
Input: Specify the true values of the parameters: Ψ.
Input: $N = 1000$ (Number of iterations).
for $i = 1$ **to** k **do**
  Generate n random samples of the covariate from the uniform distribution on the interval $(0,1)$.
  for $j = 1$ **to** N **do**
    Generate the n samples of the response variable from n NUMW distribution using its quantile function $Q_W(\tau)$.
    Estimate the parameters of the NUMWQR model: $\hat{\rho}, \hat{\vartheta}, \hat{\varsigma}, \hat{\delta}_0, \hat{\delta}_1$.
  Calculate AE, AB, RMSE, CP and AL.

The simulation study is conducted under three parameter settings. These include $R_1 : (\rho = 0.7, \vartheta = 1.2, \varsigma = 1.8, \delta_0 = 0.2, \delta_1 = 1.2)$, $R_2 : (\rho = 0.8, \vartheta = 1.2, \varsigma = 1.2, \delta_0 = 0.6, \delta_1 = -0.5)$ and $R_3 : (\rho = 1.5, \vartheta = 0.5, \varsigma = 1.5, \delta_0 = 1.3, \delta_1 = 0.2)$. For each parameter set, the quantile levels $\tau = (0.1, 0.25, 0.5, 0.75, 0.9)$ are considered in order to assess the performance of the estimators across various portions of the distribution. The results are presented in Figures 9, 10 and 11, with horizontal lines indicating the true parameter values in the AE plots. It can be observed that the AE all tend to approach the actual values while AB and RMSE become smaller as the sample sizes increase across the various quantiles. Generally, it can be observed that the CPs grow closer to the nominal 95% level as the sample size increases, and tend to hover around it for larger samples, while AL decreases. This indicates that the estimators are asymptotically consistent across the quantiles and hence are suitable for practical purposes.

6 Data Analysis

This section presents the empirical applications of NUMW distribution and NUMWQR model. The performances of the models are compared with that of other distributions.

6.1 NUMW Distribution

Three different datasets are used in this subsection. The first two datasets comprise estimates from two algorithms, P3 and SC16, which the electric utility industry uses to estimate unit capacity factors. This was recorded by [44]. The third data consists of the homicide rate from the Better Life Index (BLI) of Organisation for Economic Co-operation and Development (OECD) countries. This was obtained from https://stats.oecd.org/index.aspx?DataSetCode=BLI. Table 2 shows the numerical summaries of the datasets. It is revealed that all the datasets are positively skewed. Datasets 1 and 2 are platykurtic, while Data 3 is leptokurtic in nature.

Table 2: Numerical Summaries of Datasets

Data	Minimum	Maximum	Mean	Median	Variance	Skewness	Kurtosis
Data 1	0.0100	0.8740	0.3039	0.1180	0.1010	0.7114	1.8838
Data 2	0.0060	0.8660	0.2881	0.1160	0.1012	0.7676	1.9741
Data 3	0.0020	0.2680	0.0263	0.0085	0.0032	3.4862	14.2081

The total time on test (TTT) plots for the datasets are presented in Figure 12. The plots suggest that Data 1 and 2 are characterized by a bathtub shaped hazard rate as their TTT plots show an initial convex shape and then followed by a concave shape. Also, Data 3 is characterized by a decreasing hazard rate as its TTT plot shows a convex shape.

© 2026 NSP
Natural Sciences Publishing Cor.

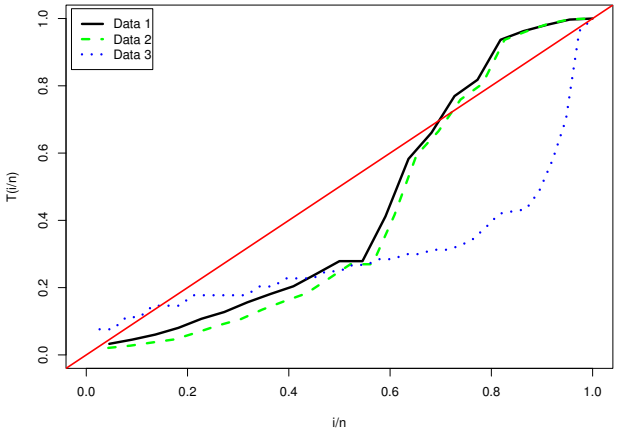


Fig. 12: TTT Plots of Data

Box plots are shown in Figure 13 for the datasets. It can be observed that data 3 has some outliers. The characteristics of the datasets suggest that the NUMW distribution will provide a good fit to them.

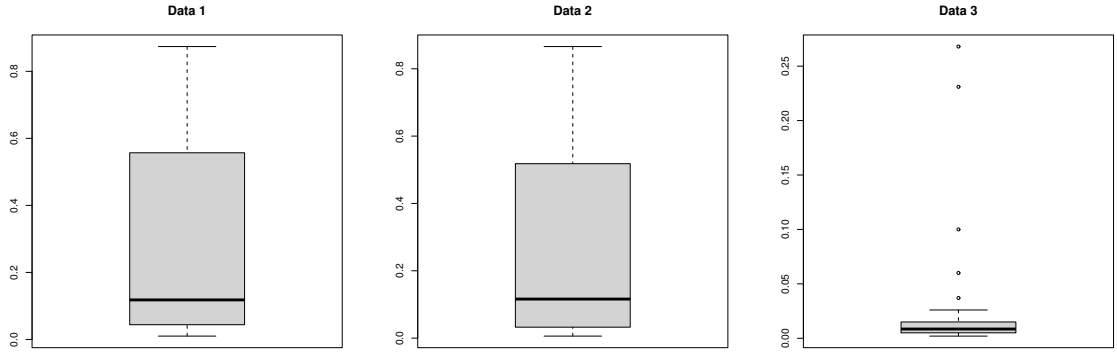


Fig. 13: Box Plots of Data

For the three datasets, the empirical performance of the NUMW distribution is compared with that of other unit distributions. These distributions include unit modified Weibull (UMW) [15], unit Weibull (UW) [5], beta, Kumaraswamy (Kum) [1], unit Lindley (UL) [6], new unit Lindley (NUL) [16], Topp-Leone (TL) [4], unit Rayleigh (UR) [7], log-cosine power (LCP) [13] distributions. They are compared via Akaike (AIC), AIC corrected (AICc) and Bayesian (BIC) information criteria, and Cramér-von Mises (CM) and Anderson-Darling (AD) goodness-of-fit measures with their associated p-values. The distribution with the smallest AIC, AICc, BIC, CM and AD statistics, with high p-values of CM and AD, is considered the best distribution for the data.

6.1.1 Data 1: P3 Algorithm Data

The distributions are fitted to Data 1 and the results presented in Table 3. The estimated parameter values, with associated standard errors (SE) in parentheses, and model fit measures are presented. The results show that NUMW distribution has the least statistic of each measure, and the highest corresponding p-values for CM and AD measures. This implies that the NUMW distribution best describes Data 1. The next best fit model is the UMW distribution.

© 2026 NSP
Natural Sciences Publishing Cor.

Table 3: Parameter Estimates and Model Fit Measures for Data 1

Distribution	Estimate (SE)	AIC	AICc	BIC	CM (p-value)	AD (p-value)
NUMW	0.7568 (0.2490)	-14.1819	-11.8290	-9.8178	0.0168 (0.9994)	0.1475 (0.9989)
	0.0870 (0.0377)					
	0.7870 (0.2470)					
	14.3613 (5.2247)					
UMW	0.2493 (0.1130)	-11.5643	-10.2310	-8.2912	0.0594 (0.8231)	0.3876 (0.8596)
	0.7120 (0.3093)					
	0.3195 (0.1804)					
UW	0.4003 (0.1263)	-10.3510	-9.7194	-8.1689	0.1208 (0.4955)	0.7511 (0.5160)
	1.2259 (0.2212)					
Beta	0.5540 (0.1423)	-9.5638	-8.9323	-7.3818	0.1264 (0.4733)	0.7241 (0.5373)
	1.2198 (0.3758)					
Kum	0.5719 (0.1478)	-9.6872	-9.0557	-7.5051	0.1231 (0.4864)	0.7175 (0.5426)
	1.2306 (0.3483)					
UL	1.1930 (0.1948)	15.1652	15.3652	16.2562	1.2694 (0.0004)	10.6345 (2.9×10^{-5})
NUL	0.1089 (0.0165)	23.3631	23.5631	24.4541	0.8844 (0.0041)	10.9450 (2.8×10^{-5})
TL	0.6778 (0.1445)	-8.9965	-8.7965	-7.9055	0.1777 (0.3166)	1.4678 (0.1845)
UR	0.1672 (0.0356)	-3.4713	-3.2713	-2.3803	0.2763 (0.1578)	3.4444 (0.0167)
LCP	0.2519 (0.0537)	-9.1706	-8.5390	-6.9885	0.1254 (0.4771)	0.7008 (0.5564)
	0.0003 (0.0194)					

The comparative performance of the fitted distributions is displayed graphically in Figure 14 using probability-probability (P–P) plots. It is evident that NUMW distribution provides the best fit to Data 1 as it best aligns along the diagonal of the plot.

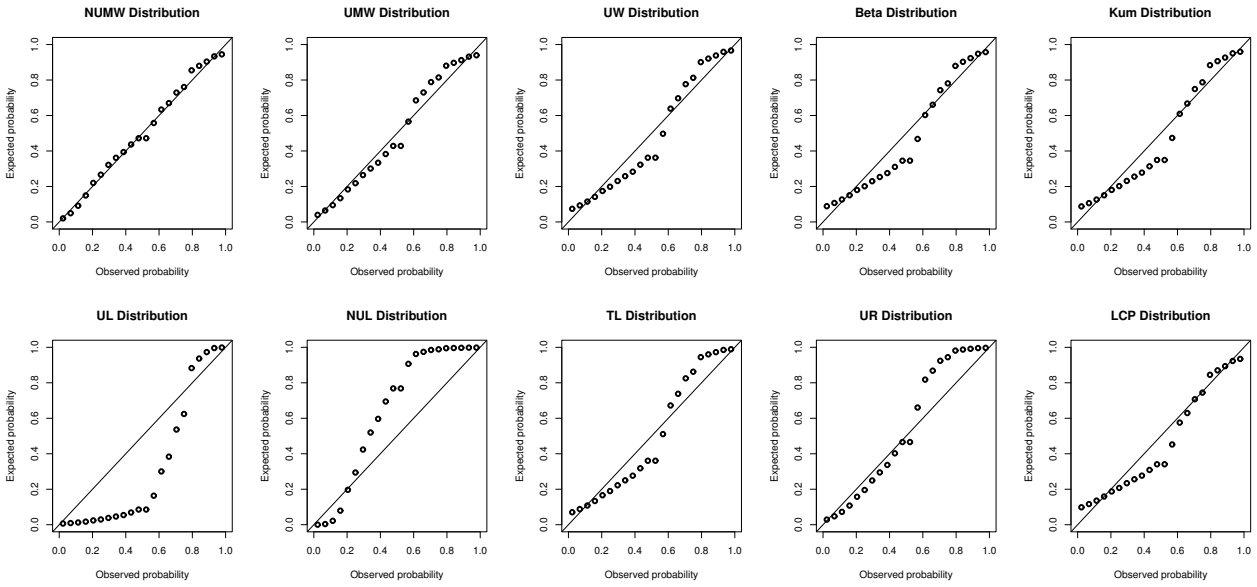


Fig. 14: P–P Plots of Fitted Distributions for Data 1

Figure 15 presents the estimated CDFs of the fitted distributions alongside the empirical CDF. The plots reveal that the estimated CDF of the NUMW distribution follows the empirical CDF more closely than those of the competing distributions, which supports the conclusion drawn from Table 3 and Figure 14.

© 2026 NSP
Natural Sciences Publishing Cor.

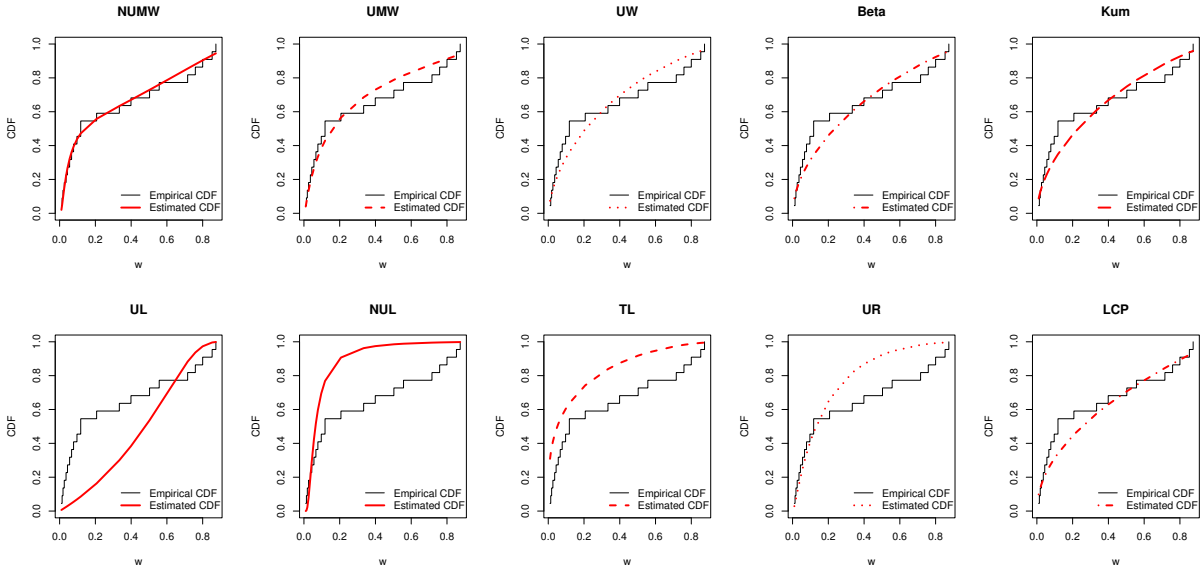


Fig. 15: CDF Plots of Fitted Distributions for Data 1

The uniqueness of the estimated parameters of the NUMW distribution is investigated using graphical tools. These include profile log-likelihood (PLL) plots and the plots of the score functions (SC). If the estimated parameters are unique and maximize the log-likelihood function, then the estimated parameter value should be the maximum on the strictly concave shape of the PLL plots. Also, the uniqueness is visible as a single downward zero-crossing of the score function, going from positive to negative. The change of the signs at the estimated value confirms the uniqueness of the maximum.

Figure 16 shows the PLL and SC plots of the estimated parameters of the NUMW distribution for Data 1. It can be observed that the estimated parameter values are indeed the maximum and are unique as they mark the maximum on the strictly concave PLL curve and the SC plots go from positive to negative, crossing at the estimated value.

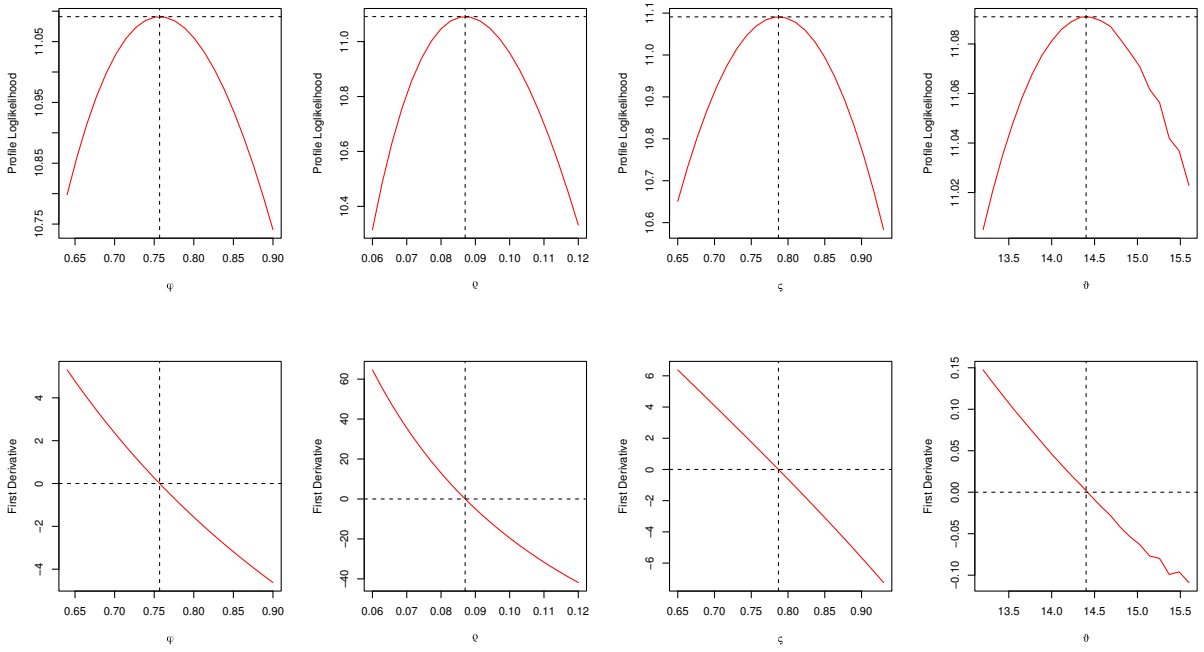


Fig. 16: PLL and SC Plots of Fitted NUMW Distribution for Data 1

© 2026 NSP
Natural Sciences Publishing Cor.

6.1.2 Data 2: SC16 Algorithm Data

The estimated parameters and model fit measures for the Data 2 are presented in Table 4. Based on the results, NUMW distribution fits the data best as it has the lowest values of all the criteria and the highest CM and AD p-values. Similar to the performance comparison of Data 1, UMW distribution provides quite a good fit to the data.

Table 4: Parameter Estimates and Model Fit Measures for Data 2

Distribution	Estimate (SE)	AIC	AICc	BIC	CM (p-value)	AD (p-value)
NUMW	0.7127 (0.2263)	-19.7745	-17.5522	-15.2325	0.0175 (0.9991)	0.1636 (0.9975)
	0.0836 (0.0312)					
	0.6383 (0.1792)					
	14.9765 (3.9775)					
UMW	0.2417 (0.1040)	-17.2493	-15.9862	-13.8429	0.0540 (0.8568)	0.3787 (0.8683)
	0.7023 (0.2933)					
	0.2766 (0.1540)					
UW	0.3645 (0.1169)	-15.9262	-15.3262	-13.6553	0.1137 (0.5254)	0.7350 (0.5287)
	1.1952 (0.2106)					
Beta	0.4869 (0.1208)	-15.2149	-14.6149	-12.9439	0.1189 (0.5031)	0.6998 (0.5573)
	1.1679 (0.3578)					
Kum	0.5044 (0.1288)	-15.3416	-14.7416	-13.0706	0.1159 (0.5157)	0.6975 (0.5592)
	1.1862 (0.3264)					
UL	1.2533 (0.2010)	15.6546	15.8450	16.7901	1.4346 (0.0002)	12.8684 (2.6×10^{-5})
NUL	0.0694 (0.0102)	35.7326	35.9231	36.8681	1.2853 (0.0004)	16.2872 (2.6×10^{-5})
TL	0.5943 (0.1239)	-14.2302	-14.0398	-13.0948	0.1735 (0.3270)	1.5271 (0.1703)
UR	0.1342 (0.0280)	-7.5045	-7.3140	-6.3690	0.2954 (0.1391)	3.8391 (0.0107)
LCP	0.2271 (0.0474)	-14.9690	-14.3690	-12.6980	0.1177 (0.5082)	0.6723 (0.5807)
	3.5×10^{-5} (0.0002)					

The superior performance of the NUMW distribution on Data 2 is confirmed using P–P plots of the fitted distributions given in Figure 17. It can be observed that NUMW distribution has its plots aligning more along the diagonal. This is closely followed by UMW distribution.

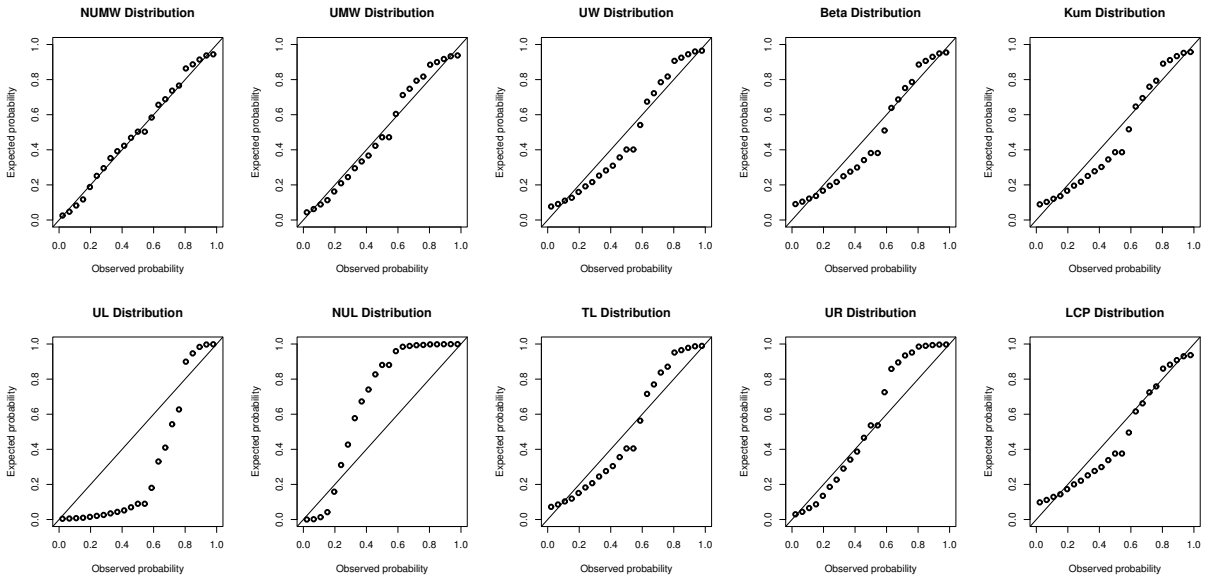


Fig. 17: P–P Plots of Fitted Distributions for Data 2

© 2026 NSP
Natural Sciences Publishing Cor.

The empirical versus estimated CDF plots of the distributions are presented in Figure 18. The estimated CDF of the NUMW distribution closely aligns with the empirical CDF. This further supports the conclusions that the NUMW distribution outperforms the competing distributions.

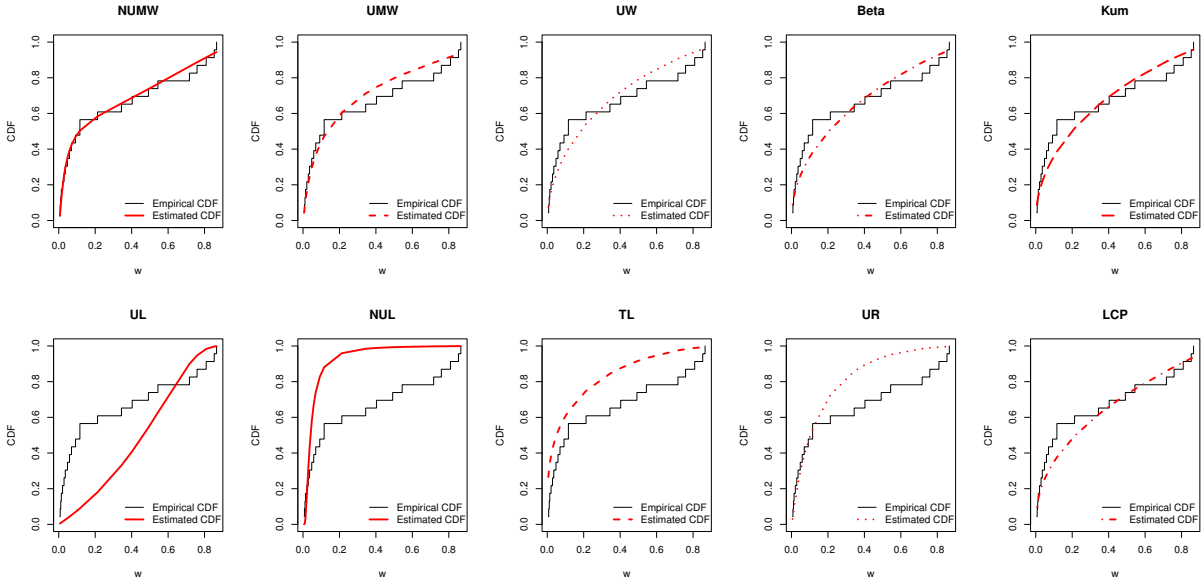


Fig. 18: CDF Plots of Fitted Distributions for Data 2

Figure 19 shows the PLL and SC plots of the parameter estimates of the NUMW distribution. It is observed that the estimated parameter values are unique and also maximize the log-likelihood function.

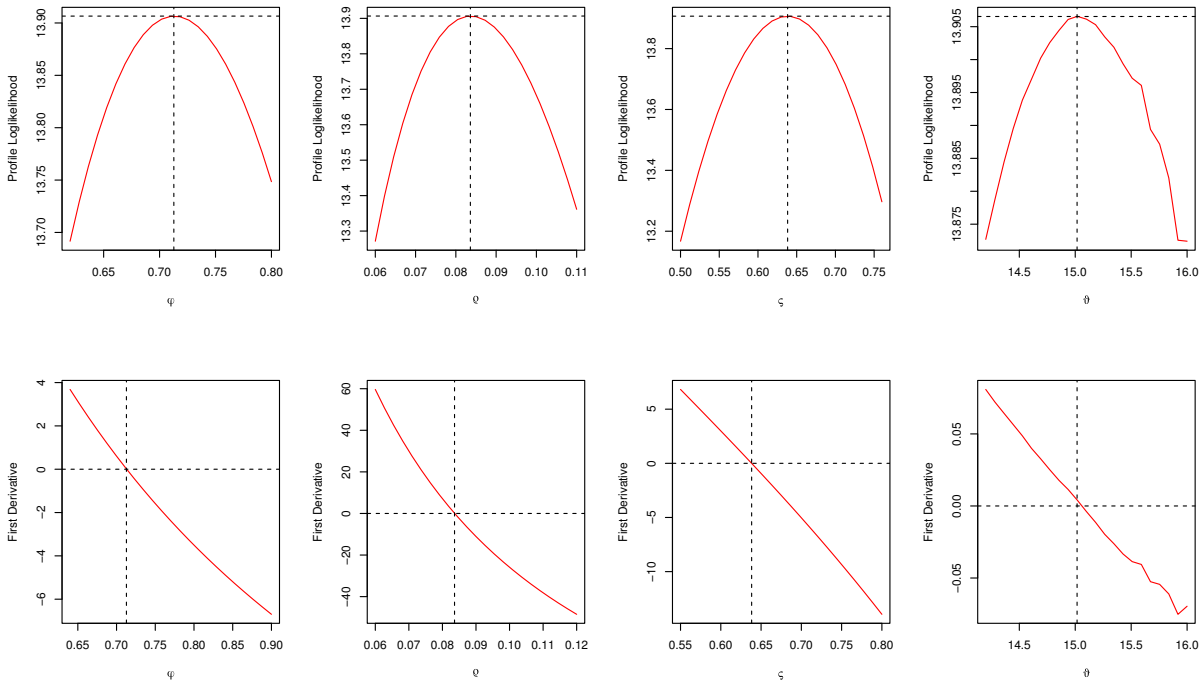


Fig. 19: PLL and SC Plots of Fitted NUMW Distribution for Data 2

© 2026 NSP
Natural Sciences Publishing Cor.

6.1.3 Data 3: Homicide Data

Table 5 presents the estimated parameters of the fitted distributions together with their corresponding model fit statistics. The NUMW distribution has the lowest values for all the measures except the BIC. For the BIC, the NUL distribution has the lowest value, followed by the UMW distribution, with the NUMW distribution ranking third. Since the BIC imposes a heavier penalty on the number of parameters, this difference is not unexpected. Considering all the other measures, the NUMW distribution provides the best fit to the data.

Table 5: Parameter Estimates and Model Fit Measures for Data 3

Distribution	Estimate (SE)	AIC	AICc	BIC	CM (p-value)	AD (p-value)
NUMW	0.1316 (0.0943)	-234.3105	-233.0983	-227.7601	0.0315 (0.9724)	0.2313 (0.9794)
	0.1504 (0.1051)					
	1.3650 (0.2821)					
	43.6178 (30.5469)					
UMW	0.0018 (0.0022)	-233.3217	-232.6159	-228.4090	0.0364 (0.9528)	0.3049 (0.9340)
	0.1579 (0.0315)					
	1.2074 (0.2162)					
UW	0.0031 (0.0061)	-223.3657	-223.0229	-220.0906	0.4976 (0.0398)	2.3832 (0.0574)
	3.6769 (1.1691)					
Beta	0.6235 (0.1206)	-199.3429	-199.0001	-196.0678	0.7967 (0.0071)	4.1382 (0.0076)
	22.0441 (6.1265)					
Kum	0.6905 (0.0841)	-204.8281	-204.4853	-201.5530	0.5579 (0.0279)	3.1610 (0.0229)
	13.9606 (4.5368)					
UL	32.9837 (5.2020)	-189.6905	-189.5794	-188.0529	1.8176 (2.3×10^{-5})	8.9771 (4.9×10^{-5})
NUL	0.0136 (0.0016)	-231.9150	-231.8039	-230.2774	0.0532 (0.8593)	0.9135 (0.4053)
TL	0.2579 (0.0418)	-164.1739	-164.0628	-162.5363	1.9206 (1.3×10^{-5})	9.2369 (4.0×10^{-5})
UR	0.0454 (0.0074)	148.5098	148.6209	150.1473	1.2367 (6.0×10^{-4})	5.9954 (0.0010)
LCP	0.1097 (0.0178)	-151.8418	-151.4989	-148.5666	2.0949 (4.5×10^{-6})	10.0609 (2.2×10^{-5})
	8.2×10^{-8} (1.2×10^{-5})					

P–P plots of the fitted distributions in Figure 20 supports the results in Table 5, as the plots for the NUMW distribution aligns more along the diagonal. Also, UMW and NUL distributions provide good fit to the data as well.

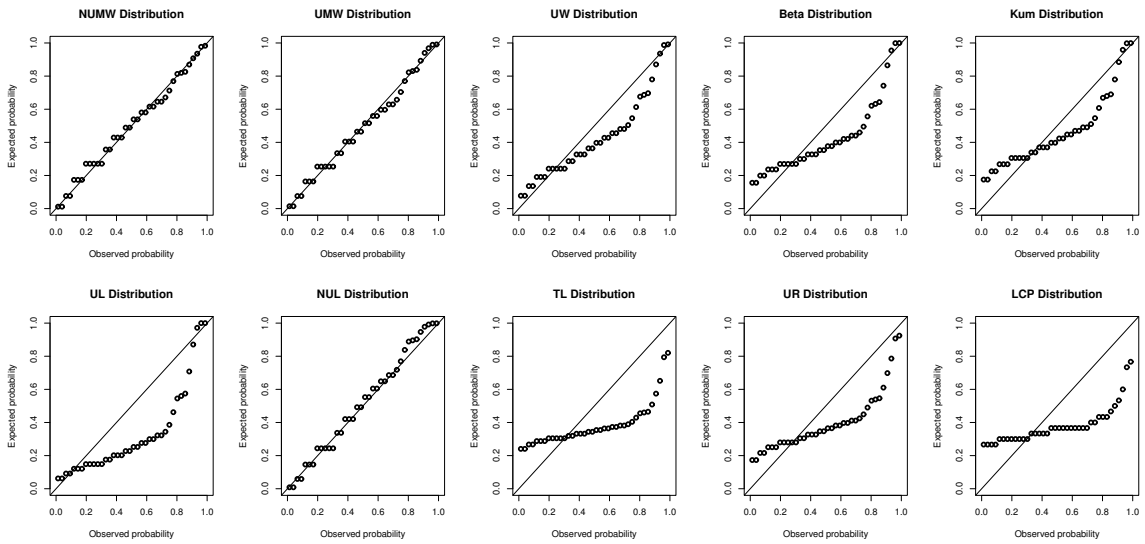


Fig. 20: P–P Plots of Fitted Distributions for Data 3

© 2026 NSP
Natural Sciences Publishing Cor.

Figure 21 illustrates the empirical versus estimated CDF plots of the fitted distributions. As concluded from Table 5 and Figure 20, it can be observed that NUMW distribution outperforms the competing distributions as its estimated CDF closely aligns with the empirical CDF.

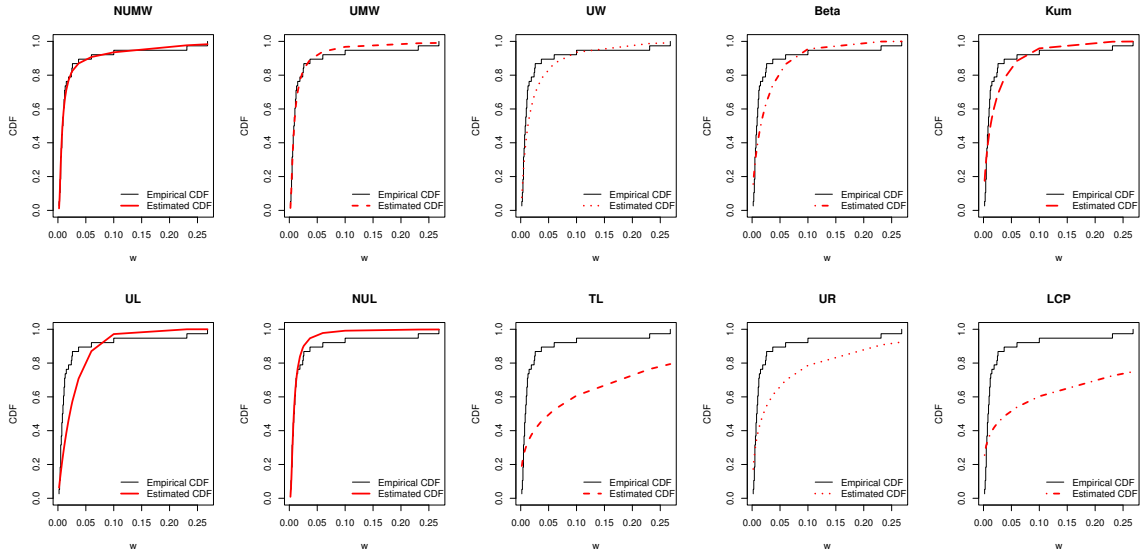


Fig. 21: CDF Plots of Fitted Distributions for Data 3

Figure 22 shows the PLL and SC plots of the estimated parameters for the NUMW distribution. It can be observed that the estimated parameter values are unique and also maximizes the log-likelihood function.

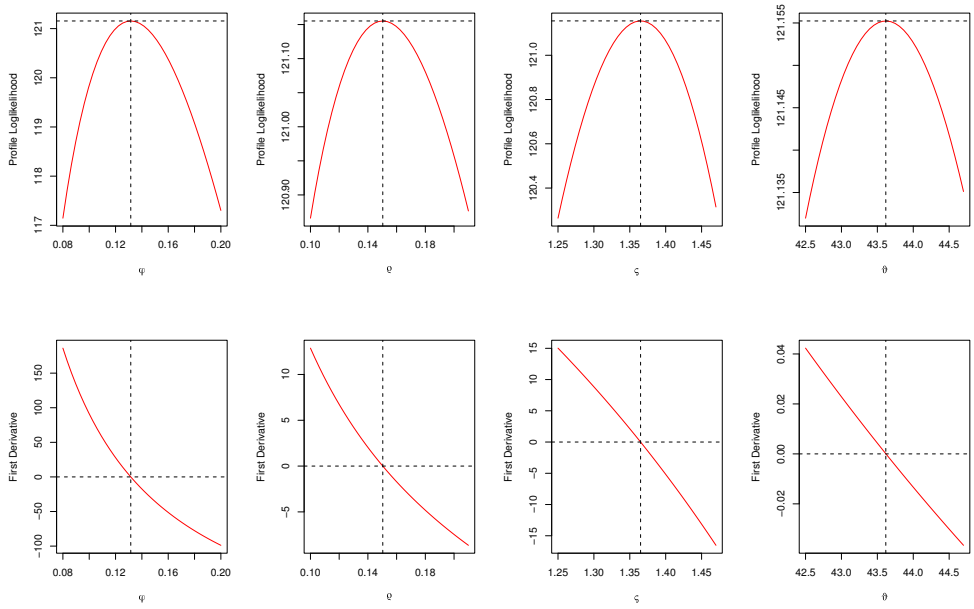


Fig. 22: PLL and SC Plots of Fitted NUMW Distribution for Data 3

© 2026 NSP
Natural Sciences Publishing Cor.

6.2 Regression Applications

To show the practical relevance of the NUMWQR model, BLI data of OECD countries, obtained from https://stats.oecd.org/index.aspx?DataSetCode=BLI, is used. Educational attainment (EA) is considered as the response variable, while life satisfaction (LS) and homicide rates (HR) serve as covariates. Numerical summaries of the data are given in Table 6. It is observed that the response variable is negatively skewed and leptokurtic in nature. For the regressors, LS is negatively skewed and platykurtic, while HR is positively skewed and leptokurtic.

Table 6: Numerical Summaries of Regression Data

Data	Minimum	Maximum	Mean	Median	Variance	Skewness	Kurtosis
EA	0.4200	0.9400	0.7903	0.8300	0.0214	-1.3483	3.8823
LS	4.9000	7.9000	6.7026	6.7500	0.4338	-0.4625	2.8303
HR	0.2000	26.8000	2.6263	0.8500	31.8955	3.4862	14.2081

The nature of the data can be confirmed from Figure 23. EA and LS can be observed to be negatively skewed while HR is positively skewed.

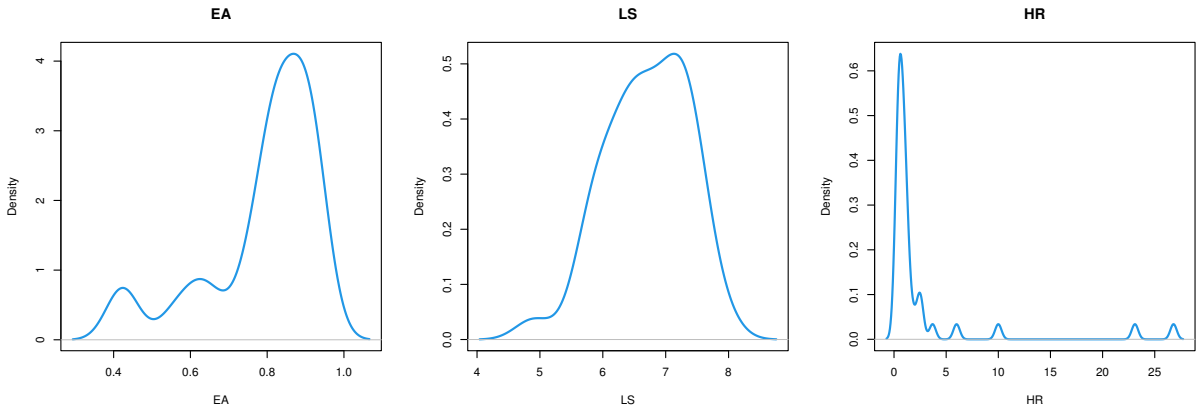


Fig. 23: Kernel Density Plots of Regression Data

Given the nature of the response variable, the NUMWQR model can be used to model it. The regression model structure used for this data is

$$\text{logit}(\eta_h) = \delta_0 + \delta_1 \text{LS}_h + \delta_2 \text{HR}_h, \quad h = 1, 2, 3, \ldots, 38.$$

How well NUMWQR model fit the data is compared with other QR models. These include Kumaraswamy QR (KQR) [30], unit-Gompertz QR (UGQR) [34], unit-Generalized Half-Normal-X QR (UGHNXQR) [32] and log-extended exponential-geometric QR (LEEGQR) [31].

The models are fitted for different quantiles $\tau = (0.10, 0.25, 0.50, 0.75, 0.90)$. The estimated QR model parameters, SEs and p-values are given in Table 7. It is observed that LS and HR are significant at 5% for NUMWQR and UGQR models across all quantiles. Also, LS is not significant at 5%, while HR is significant for KQR and UGHNXQR models across all quantiles. HR is significant for LEEGQR model across all quantiles. However, LS is only significant at 75% and 90% quantiles.

© 2026 NSP
Natural Sciences Publishing Cor.

Table 7: Estimated Parameters, Standard Errors, and p-values of Fitted QR Models

τ	Metric	ρ / θ	ϑ	ς	δ_0	δ_1	δ_2
Panel A: NUMWQR Model $(\rho, \vartheta, \varsigma, \delta_0, \delta_1, \delta_2)$							
	Estimate	0.1698	11.7259	265.7647	-3.4492	0.6209	-0.0267
0.10	SE	0.0240	0.6939	0.0013	0.7017	0.1075	0.0084
	p-value	< 0.0001	< 0.0001	< 0.0001	< 0.0001	< 0.0001	0.0015
	Estimate	0.1742	11.6062	241.5165	-2.7809	0.5773	-0.0383
0.25	SE	0.0287	1.4980	0.0119	1.4674	0.2063	0.0152
	p-value	< 0.0001	< 0.0001	< 0.0001	0.0581	0.0051	0.0115
	Estimate	0.2114	9.6219	81.0175	-1.8898	0.5134	-0.0479
0.50	SE	0.0369	1.3759	0.0293	1.0648	0.1522	0.0181
	p-value	< 0.0001	< 0.0001	< 0.0001	0.0759	0.0007	0.0082
	Estimate	0.2284	8.9121	61.9251	-1.1980	0.4858	-0.0477
0.75	SE	0.0422	1.4073	0.0386	0.9833	0.1408	0.0239
	p-value	< 0.0001	< 0.0001	< 0.0001	0.2231	0.0006	0.0460
	Estimate	0.2169	9.3681	87.3074	-0.5516	0.4702	-0.0436
0.90	SE	0.0357	1.2343	0.0245	0.3141	0.0523	0.0194
	p-value	< 0.0001	< 0.0001	< 0.0001	0.0791	< 0.0001	0.0245
Panel B: KQR Model $(\theta, \delta_0, \delta_1, \delta_2)$							
	Estimate	1.9987	—	—	0.1368	0.0788	-0.0419
0.10	SE	0.1756	—	—	0.8618	0.1228	0.0097
	p-value	< 0.0001	—	—	0.8739	0.5213	< 0.0001
	Estimate	2.0070	—	—	0.4399	0.1001	-0.0501
0.25	SE	0.1761	—	—	1.0892	0.1576	0.0113
	p-value	< 0.0001	—	—	0.6863	0.5253	< 0.0001
	Estimate	2.0161	—	—	0.7589	0.1298	-0.0615
0.50	SE	0.1765	—	—	1.4320	0.2093	0.0136
	p-value	< 0.0001	—	—	0.5961	0.5350	< 0.0001
	Estimate	2.0249	—	—	1.0936	0.1629	-0.0756
0.75	SE	0.1767	—	—	1.8707	0.2751	0.0165
	p-value	< 0.0001	—	—	0.5588	0.5537	< 0.0001
	Estimate	2.0330	—	—	1.4651	0.1894	-0.0914
0.90	SE	0.1769	—	—	2.3368	0.3452	0.0196
	p-value	< 0.0001	—	—	0.5307	0.5833	< 0.0001
Panel C: UGQR Model $(\theta, \delta_0, \delta_1, \delta_2)$							
	Estimate	1.2528	—	—	-3.1285	0.5694	-0.0380
0.10	SE	0.2828	—	—	0.9185	0.1375	0.0146
	p-value	< 0.0001	—	—	0.0007	< 0.0001	0.0096
	Estimate	1.2502	—	—	-3.1557	0.6246	-0.0410
0.25	SE	0.2822	—	—	1.0101	0.1502	0.0157
	p-value	< 0.0001	—	—	0.0018	< 0.0001	0.0092
	Estimate	1.2433	—	—	-3.1484	0.7013	-0.0459
0.50	SE	0.2833	—	—	1.1759	0.1708	0.0176
	p-value	< 0.0001	—	—	0.0074	< 0.0001	0.0092
	Estimate	1.2345	—	—	-2.9591	0.7841	-0.0533
0.75	SE	0.2842	—	—	1.4248	0.2001	0.0206
	p-value	< 0.0001	—	—	0.0378	0.0001	0.0098
	Estimate	1.2271	—	—	-2.4076	0.8411	-0.0620
0.90	SE	0.2788	—	—	1.6190	0.2231	0.0249
	p-value	< 0.0001	—	—	0.1370	0.0002	0.0128
Panel D: UGHNXQR Model $(\theta, \delta_0, \delta_1, \delta_2)$							
	Estimate	0.2034	—	—	0.4042	0.0129	-0.0729
0.10	SE	0.1328	—	—	1.3509	0.1912	0.0274
	p-value	0.1257	—	—	0.7648	0.9462	0.0077
	Estimate	0.2034	—	—	1.1633	0.0129	-0.0729
0.25	SE	0.1323	—	—	1.2750	0.1837	0.0256
	p-value	0.1242	—	—	0.3616	0.9439	0.0043
	Estimate	0.2035	—	—	1.7744	0.0130	-0.0729
0.50	SE	0.1315	—	—	1.2358	0.1800	0.0242

Continued on next page

© 2026 NSP
Natural Sciences Publishing Cor.

Table 7 – *Continued from previous page*

τ	Metric	ρ / θ	ϑ	ς	δ_0	δ_1	δ_2
	p-value	0.1219	—	—	0.1510	0.9423	0.0025
	Estimate	0.2034	—	—	2.2114	0.0128	-0.0729
0.75	SE	0.1313	—	—	1.2178	0.1782	0.0233
	p-value	0.1212	—	—	0.0694	0.9426	0.0017
	Estimate	0.2034	—	—	2.5030	0.0128	-0.0729
0.90	SE	0.1312	—	—	1.2096	0.1774	0.0228
	p-value	0.1211	—	—	0.0385	0.9423	0.0014
Panel E: LEEGQR Model $(\theta, \delta_0, \delta_1, \delta_2)$							
	Estimate	2.1075	—	—	-1.3630	0.2959	-0.0361
0.10	SE	0.2141	—	—	1.2631	0.1812	0.0129
	p-value	< 0.0001	—	—	0.2805	0.1025	0.0050
	Estimate	2.1120	—	—	-1.5880	0.3910	-0.0406
0.25	SE	0.2127	—	—	1.5314	0.2223	0.0147
	p-value	< 0.0001	—	—	0.2997	0.0786	0.0058
	Estimate	2.1200	—	—	-2.0232	0.5338	-0.0470
0.50	SE	0.2111	—	—	1.8875	0.2749	0.0174
	p-value	< 0.0001	—	—	0.2838	0.0522	0.0069
	Estimate	2.1281	—	—	-2.4241	0.6939	-0.0575
0.75	SE	0.2138	—	—	2.3347	0.3360	0.0213
	p-value	< 0.0001	—	—	0.2991	0.0389	< 0.0001
	Estimate	2.1185	—	—	-1.8443	0.7386	-0.0782
0.90	SE	0.2166	—	—	2.5639	0.3651	0.0245
	p-value	< 0.0001	—	—	0.4719	0.0431	0.0014

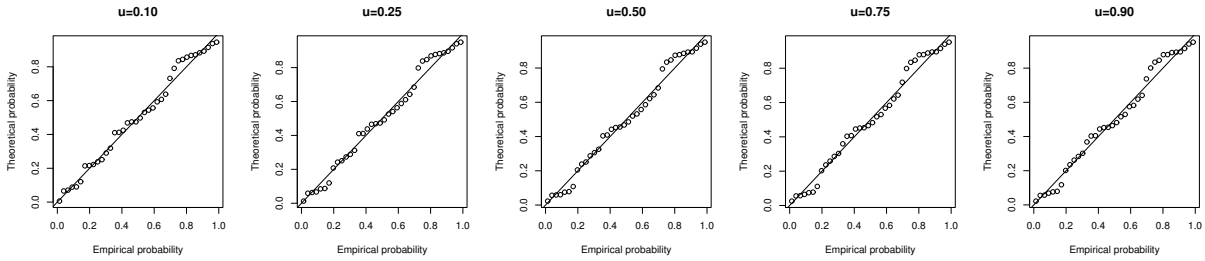
The performance of the models are compared and presented in Table 8. It can be observed that for each quantile, NUMWQR model outperformed the other models as it has the least AIC and BIC, while having the highest estimated log-likelihood value. Thus, the NUMWQR model best describes the data at the 90% quantile across all quantiles.

Table 8: Model fit Measures of Fitted Regression Models

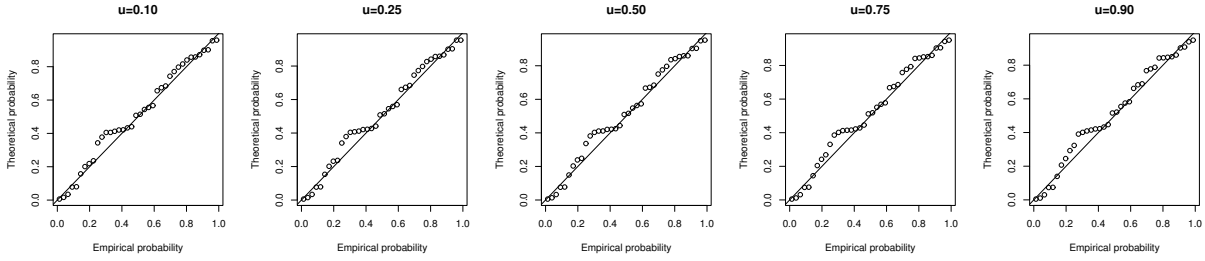
Quantile	Model	LL	AIC	BIC
0.1	NUMWQR	38.3117	-64.6234	-54.7979
	KQR	33.1044	-58.2087	-51.6584
	UGQR	33.2506	-58.5012	-51.9508
	UGHNXQR	34.5865	-61.1729	-54.6226
	LEEGQR	31.0231	-54.0462	-47.4958
0.25	NUMWQR	38.2302	-64.4603	-54.6348
	KQR	33.2466	-58.4932	-51.9428
	UGQR	33.2239	-58.4479	-51.8975
	UGHNXQR	34.5865	-61.1729	-54.6226
	LEEGQR	31.0974	-54.1948	-47.6444
0.5	NUMWQR	38.2883	-64.5766	-54.7511
	KQR	33.4016	-58.8033	-52.2529
	UGQR	33.1733	-58.3467	-51.7963
	UGHNXQR	34.5865	-61.1729	-54.6226
	LEEGQR	31.1470	-54.2939	-47.7436
0.75	NUMWQR	38.3777	-64.7554	-54.9299
	KQR	33.5449	-59.0898	-52.5394
	UGQR	33.1075	-58.2150	-51.6647
	UGHNXQR	34.5865	-61.1729	-54.6226
	LEEGQR	31.0961	-54.1922	-47.6419
0.9	NUMWQR	38.5269	-65.0538	-55.2283
	KQR	33.6626	-59.3252	-52.7748
	UGQR	33.0637	-58.1274	-51.5771
	UGHNXQR	34.5865	-61.1729	-54.6226
	LEEGQR	30.9411	-53.8822	-47.3319

Figure 24 shows the CSR plots for all the fitted distributions. It is observed that NUMWQR model provides the best fit to the data at $\tau = 90\%$.

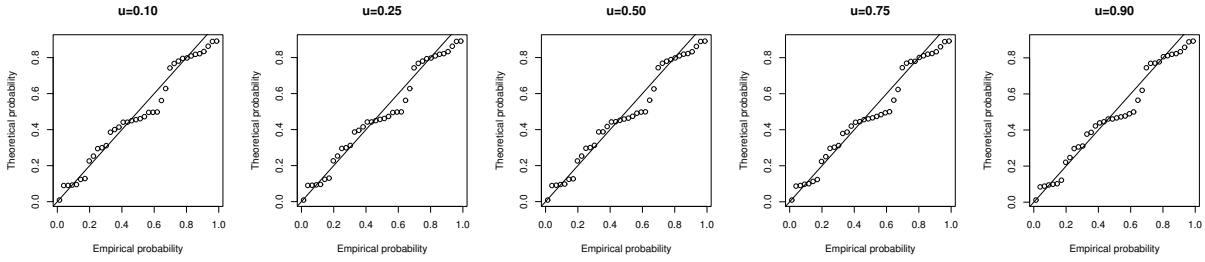
© 2026 NSP
Natural Sciences Publishing Cor.



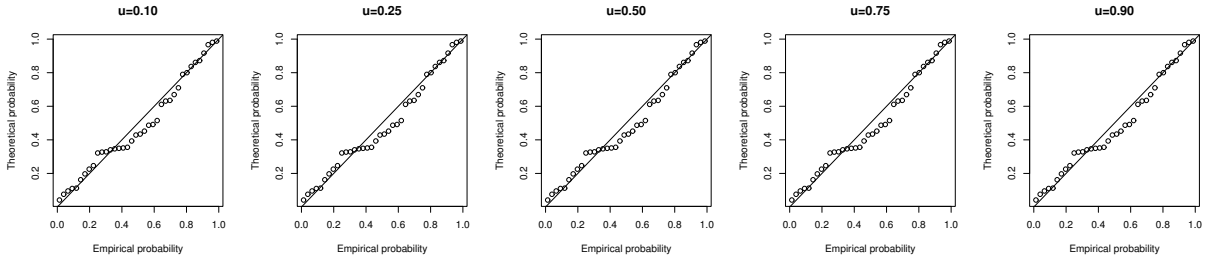
(a) NUMWQR



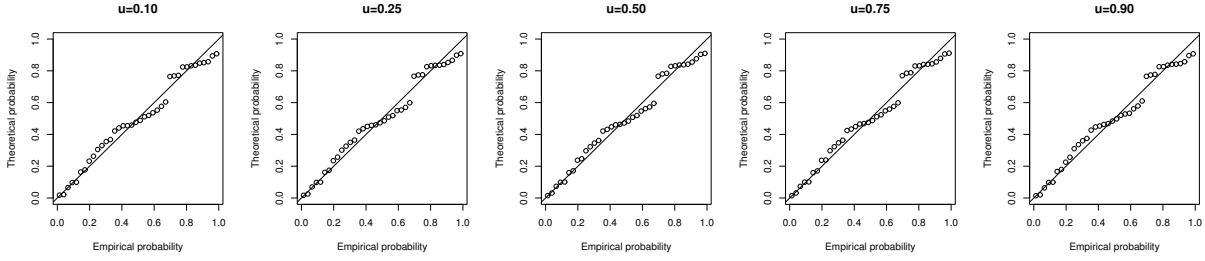
(b) KQR



(c) UGQR



(d) UGHNXQR



(e) LEEGQR

Fig. 24: P–P Plots of CSR of Fitted Regression Models

© 2026 NSP
Natural Sciences Publishing Cor.

Figure 25 shows the PLL of estimated parameters of the fitted NUMWQR model at 90% quantile. It is evident that the estimated parameters of the model are unique and the maximum.

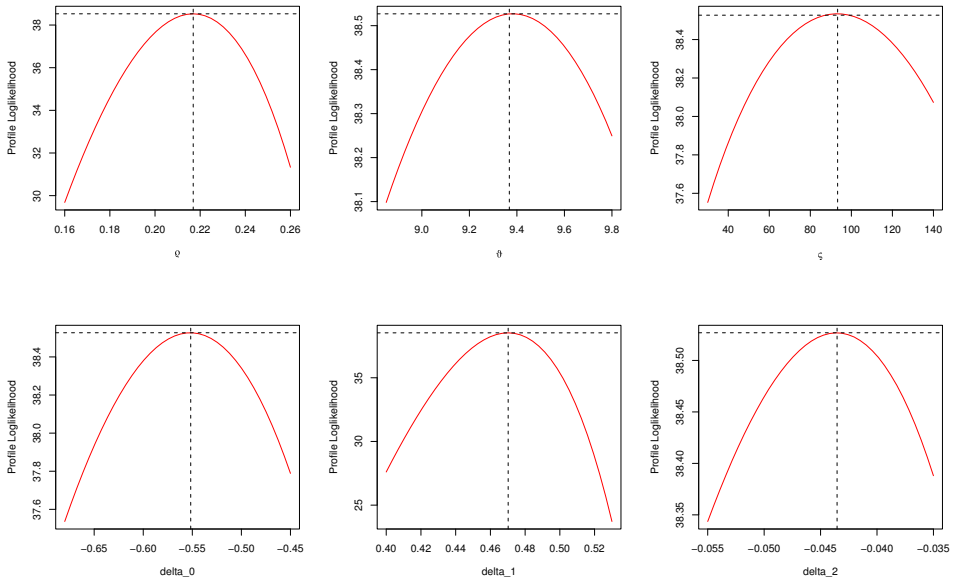


Fig. 25: PLL Plots of Estimated Parameters of NUMWQR Model

7 Conclusion

This study proposed a unit distribution, referred to as the novel unit modified Weibull (NUMW) distribution. The NUMW distribution was developed to provide a flexible alternative distribution for modeling unit interval data. Using various properties of the distribution, it was shown that the distribution exhibits monotone increasing and decreasing, left and right skewed density shapes. Again, monotone increasing and decreasing, bathtub and modified bathtub hazard shapes were also obtained. Maximum likelihood technique was used for parameter estimation of the new unit distribution. Assessment of the estimators of the parameters via Monte Carlo simulations show that the estimators are asymptotically consistent. To accommodate covariates with the response variable exhibiting the presence of outliers and extreme skewness, a QR model is developed for responses following the NUMW distribution. Using real-life datasets, the empirical relevance of the NUMW distribution and its regression model are demonstrated, and their performance compared with other models. The results revealed that the new bounded distribution and its corresponding regression model provide competitive alternative models to data on the unit interval.

Some limitations of the distribution are acknowledged and recommendations provided for future work. Firstly, the simulation study shows a sample bias towards small samples for some of the parameters. Also, the shape parameter ϑ is observed to be estimated with large standard errors in the application section. Secondly, the moments and inequality measures have no closed-form and must be computed numerically. Thirdly, only maximum likelihood estimation was considered in the study. Future work could consider Bayesian or other frequentist estimators to address the possible estimation biases. Also, the model could be extended to model censored observations and longitudinal data. Finally, multivariate versions of the distribution could also be explored.

Availability of data and materials

The data used in this study are available from the sources cited in the article.

© 2026 NSP
Natural Sciences Publishing Cor.

Competing interests

The author declares no competing interests with respect to this study.

Funding

The author declare that no funding was received for conducting this study.

Acknowledgement

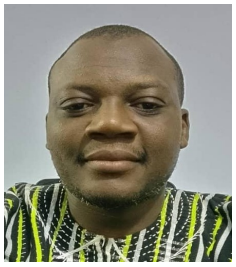
The author is grateful to the editor and the anonymous reviewers for their careful reading and constructive comments, which have improved the quality of this paper.

References

[1] Kumaraswamy, P. (1980). A generalized probability density function for double-bounded random processes. *Journal of Hydrology*, *46*, 79–88.
[2] Consul, P. C., & Jain, G. C. (1971). On the log-gamma distribution and its properties. *Statistische Hefte*, *12*, 100–106.
[3] Grassia, A. (1977). On a family of distributions with argument between 0 and 1 obtained by transformation of the gamma and derived compound distributions. *Australian Journal of Statistics*, *19*, 108-114.
[4] Topp, C. W., & Leone, F. C. (1955). A family of J-shaped frequency functions. *Journal of the American Statistical Association*, *50*, 209–219.
[5] Mazucheli, J., Menezes, A., & Ghitany, M. E. (2018). The unit-Weibull distribution and associated inference. *Journal of Applied Probability and Statistics*, *13*, 1–22.
[6] Mazucheli, J., Menezes, A. F. B., & Chakraborty, S. (2019). On the one parameter unit-Lindley distribution and its associated regression model for proportion data. *Journal of Applied Statistics*, *46*, 700–714.
[7] Bantan, R. A., Chesneau, C., Jamal, F., Elgarhy, M., Tahir, M. H., Ali, A., Zubair, M., & Anam, S. (2020). Some new facts about the unit-Rayleigh distribution with applications. *Mathematics*, *8*, 1954.
[8] Korkmaz, M. Ç. (2020). The unit generalized half normal distribution: A new bounded distribution with inference and application. *UPB Scientific Bulletin, Series A: Applied Mathematics and Physics*, *82*, 133–140.
[9] Altun, E. (2021). The log-weighted exponential regression model: Alternative to the beta regression model. *Communications in Statistics – Theory and Methods*, *50*, 2306–2321.
[10] Abubakari, A. G., Luguterah, A., & Nasiru, S. (2022). Unit exponentiated Fréchet distribution: Actuarial measures, quantile regression and applications. *Journal of the Indian Society for Probability and Statistics*, *23*, 387–424.
[11] Sapkota, L. P., Bam, N., & Kumar, V. (2025). New bounded unit Weibull model: Applications with quantile regression. *PLOS ONE*, *20*. https://doi.org/10.1371/journal.pone.0323888.
[12] Ogumeyo, S. A., Opone, F. C., Abubakari, A. G., & Ehiwario, J. C. (2024). A bounded lifetime distribution specified by a trigonometric function: Properties, regression model, and applications. *International Journal of Mathematics and Mathematical Sciences*. https://doi.org/10.1155/2024/5583105
[13] Nasiru, S., Chesneau, C., & Ocloo, S. K. (2024). The log-cosine-power unit distribution: A new unit distribution for proportion data analysis. *Decision Analytics Journal*. https://doi.org/10.1016/j.dajour.2024.100397
[14] Abubakari, A. G., Nasiru, S., & Chesneau, C. (2024). A unit Weibull loss distribution with quantile regression and practical applications to actuarial science. *Operations Research and Decisions*, *34*, 1–39.
[15] Scrimini, J. I., Bisognin, C., Guerra, R. R., & Bayer, F. M. (2025). Unit-modified Weibull distribution and quantile regression model. *Anais da Academia Brasileira de Ciências*. https://doi.org/10.1590/0001-3765202520250352
[16] Bam, N., & Sapkota, L. P. (2025). New unit Lindley mixed model: Applications to COVID-19 and child mortality rates under the Bayesian approach. *Health Services and Outcomes Research Methodology*, 1–27.
[17] Abd El-Bar, A. M. T., El-Saeed, A. R., & Gemeay, A. M. (2025). A bounded Lindley exponential model with applications to industrial engineering and epidemiological data. *AIMS Mathematics*, *10*, 16233–16263.
[18] Alomair, M. A., & Ahsan-ul Haq, M. (2026). Power unit Haq distribution: A flexible probability model for lifetime data analysis. *Mathematical Sciences*, *20*, 163–190.
[19] Jamal, F., Abd Elgawad, M. A., Imran, M., & Mohammad, S. (2026). A novel distribution on the unit interval with properties and applications for electronic components. *Axioms*. https://doi.org/10.3390/axioms15050359
[20] Nasiru, S., & Olaomi, J. O. (2026). Power-transformed Bradford distribution: Properties, quantile regression, and empirical illustrations. *Journal of Mathematics*. https://doi.org/10.1155/jom/7754935
[21] Gemeay, A. M., Elbatal, I., Almetwally, E. M., Bashiru, S. O., et al. (2025). Statistical modeling with a novel distribution: Inference, information measures, and applications to inflation rates and mechanical failure data. *AIMS Mathematics*, *10*, 19357–19394.

© 2026 NSP
Natural Sciences Publishing Cor.

[22] Bashiru, S. O., Kayid, M., Sayed, R. M., Balogun, O. S., Abd El-Raouf, M. M., & Gemeay, A. M. (2025). Introducing the unit Zeghdoudi distribution as a novel statistical model for analyzing proportional data. *Journal of Radiation Research and Applied Sciences*. https://doi.org/10.1016/j.jrras.2024.101204
[23] Al-Olaimat, N. M., Migdadi, H. S., Saadeh, R., & Hafez, M. (2026). On the two-parameter unit power Rayleigh distribution: Properties, inference and applications. *Results in Control and Optimization*. https://doi.org/10.1016/j.rico.2026.100734
[24] Gemeay, A. M., Alqasem, O. A., Khogeer, H. A., Alrumayh, A., Husseiny, I. A., & Abdelsalam, E. M. (2026). Transmuted unit new XLindley distribution: Statistical properties, parameter estimation, and applications to bounded data. *Boundary Value Problems*. https://doi.org/10.1186/s13661-026-02326-5
[25] Helal, T. S., Elbarkawy, M. A. F., Zafar, J., & Hydara, A. (2026). The unit Komal distribution: Bathtub risk function and applications. *Computational Journal of Mathematical and Statistical Sciences*. https://doi.org/10.21608/cjmss.2026.491712.1425
[26] El-Morshedy, M., Harpy, M. H., Ahsan-ul-Haq, M., & Elgarhy, M. (2026). Unit ZLindley distribution with statistical properties, estimation, and application to engineering data, *15*, 1071–1089.
[27] Bashiru, S. O., Isa, A. M., Ali, I., Arum, K. C., Oranye, H. E., Ugah, T. E., & Okoacha, N. G. (2025). Unit probability distributions: A comprehensive review of models, properties, and applications. *FUDMA Journal of Sciences*, *9*, 126–132.
[28] Lai, C. D., Xie, M., & Murthy, D. N. P. (2003). A modified Weibull distribution. *IEEE Transactions on Reliability*, *52*, 33–37.
[29] Koenker, R., & Bassett, G., Jr. (1978). Regression quantiles. *Econometrica*, *46*, 33–50.
[30] Mitnik, P. A., & Baek, S. (2013). The Kumaraswamy distribution: Median-dispersion re-parameterizations for regression modeling and simulation-based estimation. *Statistical Papers*, *54*, 177–192.
[31] Jodrá, P., & Jiménez-Gamero, M. D. (2020). *A quantile regression model for bounded responses based on the exponential-geometric distribution* [Technical report].
[32] Bakouch, H. S., Nik, A. S., Asgharzadeh, A., & Salinas, H. S. (2021). A flexible probability model for proportion data: Unit-half-normal distribution. *Communications in Statistics: Case Studies, Data Analysis and Applications*, *7*, 271–288.
[33] Mazucheli, J., Alves, B., Korkmaz, M. Ç., & Leiva, V. (2022). Vasicek quantile and mean regression models for bounded data: New formulation, mathematical derivations, and numerical applications. *Mathematics*. https://doi.org/10.3390/math10091389
[34] Mazucheli, J., Alves, B., & Korkmaz, M. Ç. (2023). The unit-Gompertz quantile regression model for the bounded responses. *Mathematica Slovaca*, *73*, 1039–1054.
[35] Alqasem, O. A., Gemeay, A. M., Alnagar, D. K., Khogeer, H. A., Alrumayh, A., Hussam, E., Gellow, G. T., & Hammad, A. T. (2026). A new quantile regression model for bounded responses: Mathematical derivation, estimation, and fitting bounded datasets. *Boundary Value Problems*. https://doi.org/10.1186/s13661-026-02369-8
[36] Arslan, T., & Yu, K. (2025). The unit-Cauchy quantile regression model with variates observed on (0, 1): Percentages, proportions, and fractions. *Hacettepe Journal of Mathematics and Statistics*, 1–23.
[37] Hamoodi, A. S., & Salih, A. M. (2026). Novel quantile regression model using extended exponential-geometric distribution with real data application. *Statistics, Optimization & Information Computing*, *16*, 660–683.
[38] Salih, A., & Al-Majidi, A. J. (2026). A flexible unit Chen quantile regression model for bounded response data: Estimation, model diagnostics, and applications. *TWMS Journal of Applied and Engineering Mathematics*, *16*, 1234–1254.
[39] El-Alosey, A. R., Hammad, A. T., & Gemeay, A. M. (2026). A novel unit exponential regression model with improved estimation method under multicollinearity. *Computational Statistics*. https://doi.org/10.1007/s00180-026-01741-7
[40] Gradshteyn, I. S., & Ryzhik, I. M. (2014). *Table of integrals, series, and products* (8th ed.). Academic Press.
[41] Gastwirth, J. L. (1972). The estimation of the Lorenz curve and Gini index. *The Review of Economics and Statistics*, *54*, 306–316.
[42] R Core Team. (2025). *R: A language and environment for statistical computing*. R Foundation for Statistical Computing. https://www.R-project.org/
[43] Cox, D. R., & Snell, E. J. (1968). A general definition of residuals. *Journal of the Royal Statistical Society: Series B (Methodological)*, *30*, 248–265.
[44] Caramanis, M., Stremel, J., Fleck, W., & Daniel, S. (1983). Probabilistic production costing: An investigation of alternative algorithms. *International Journal of Electrical Power & Energy Systems*, *5*, 75–86.



Abdul Ghaniyyu Abubakari is a Senior Lecturer at the Department of Applied Statistics, University of Business and Integrated Development Studies, Ghana. He received a PhD degree in Statistics from the University of Technology and Applied Sciences, Ghana. Broadly, his research interests are in the areas of probability theory, actuarial science, extreme value theory and machine learning. Specifically, he has experience in the development of new probability distributions, actuarial risk measures, quantile regression models and hybrid machine learning models. He has published research articles in reputable international journals of statistical and mathematical sciences. He is also a reviewer for several statistics and mathematics journals.

© 2026 NSP
Natural Sciences Publishing Cor.